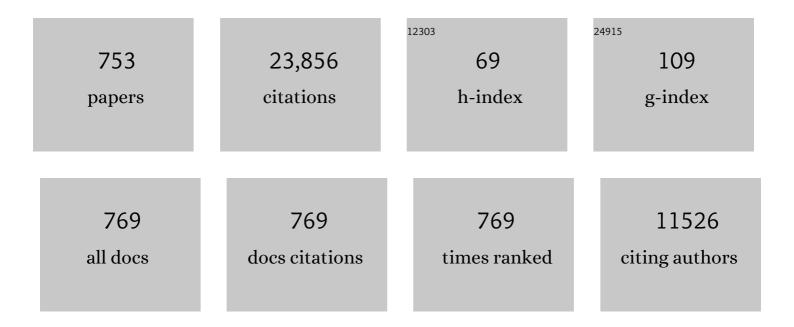
Hyoung Seop Kim

List of Publications by Year in descending order

Source: https://exaly.com/author-pdf/3906526/publications.pdf Version: 2024-02-01



#	Article	IF	CITATIONS
1	Heterostructured materials: superior properties from hetero-zone interaction. Materials Research Letters, 2021, 9, 1-31.	4.1	505
2	Fast and fully-scalable synthesis of reduced graphene oxide. Scientific Reports, 2015, 5, 10160.	1.6	486
3	Plastic deformation behaviour of fine-grained materials. Acta Materialia, 2000, 48, 493-504.	3.8	307
4	Cryogenic strength improvement by utilizing room-temperature deformation twinning in a partially recrystallized VCrMnFeCoNi high-entropy alloy. Nature Communications, 2017, 8, 15719.	5.8	278
5	Highâ€Entropy Alloys: Potential Candidates for Highâ€Temperature Applications – An Overview. Advanced Engineering Materials, 2018, 20, 1700645.	1.6	270
6	High-entropy alloys with heterogeneous microstructure: Processing and mechanical properties. Progress in Materials Science, 2022, 123, 100709.	16.0	270
7	On the rule of mixtures for the hardness of particle reinforced composites. Materials Science & Engineering A: Structural Materials: Properties, Microstructure and Processing, 2000, 289, 30-33.	2.6	261
8	On the die corner gap formation in equal channel angular pressing. Materials Science & Engineering A: Structural Materials: Properties, Microstructure and Processing, 2000, 291, 86-90.	2.6	247
9	Boron doped ultrastrong and ductile high-entropy alloys. Acta Materialia, 2018, 151, 366-376.	3.8	230
10	Dislocation density-based modeling of deformation behavior of aluminium under equal channel angular pressing. Materials Science & Engineering A: Structural Materials: Properties, Microstructure and Processing, 2003, 351, 86-97.	2.6	207
11	Novel Co-rich high performance twinning-induced plasticity (TWIP) and transformation-induced plasticity (TRIP) high-entropy alloys. Scripta Materialia, 2019, 165, 39-43.	2.6	200
12	The effects of grain size and porosity on the elastic modulus of nanocrystalline materials. Scripta Materialia, 1999, 11, 361-367.	0.5	190
13	Strain partitioning and mechanical stability of retained austenite. Scripta Materialia, 2010, 63, 297-299.	2.6	180
14	Additional hardening in harmonic structured materials by strain partitioning and back stress. Materials Research Letters, 2018, 6, 261-267.	4.1	179
15	Exceptional phase-transformation strengthening of ferrous medium-entropy alloys at cryogenic temperatures. Acta Materialia, 2018, 161, 388-399.	3.8	174
16	Tensile deformation behavior and deformation twinning of an equimolar CoCrFeMnNi high-entropy alloy. Materials Science & Engineering A: Structural Materials: Properties, Microstructure and Processing, 2017, 689, 122-133.	2.6	166
17	Micromechanical finite element analysis of strain partitioning in multiphase medium manganese TWIP+TRIP steel. Acta Materialia, 2016, 108, 219-228.	3.8	165
18	Structure and properties of ultrafine-grained CoCrFeMnNi high-entropy alloys produced by mechanical alloying and spark plasma sintering. Journal of Alloys and Compounds, 2017, 698, 591-604.	2.8	165

#	Article	IF	CITATIONS
19	Strain rate effects of dynamic compressive deformation on mechanical properties and microstructure of CoCrFeMnNi high-entropy alloy. Materials Science & Engineering A: Structural Materials: Properties, Microstructure and Processing, 2018, 719, 155-163.	2.6	163
20	High-pressure torsion for enhanced atomic diffusion and promoting solid-state reactions in the aluminum–copper system. Acta Materialia, 2013, 61, 3482-3489.	3.8	159
21	Effects of Al addition on deformation and fracture mechanisms in two high manganese TWIP steels. Materials Science & Engineering A: Structural Materials: Properties, Microstructure and Processing, 2011, 528, 2922-2928.	2.6	157
22	Tubular channel angular pressing (TCAP) as a novel severe plastic deformation method for cylindrical tubes. Materials Letters, 2011, 65, 3009-3012.	1.3	153
23	Finite element analysis of equal channel angular pressing using a round corner die. Materials Science & Engineering A: Structural Materials: Properties, Microstructure and Processing, 2001, 315, 122-128.	2.6	145
24	Novel Co-rich high entropy alloys with superior tensile properties. Materials Research Letters, 2019, 7, 82-88.	4.1	139
25	Microstructure and corrosion properties of ultrafine-grained interstitial free steel. Materials Science & Engineering A: Structural Materials: Properties, Microstructure and Processing, 2007, 462, 243-247.	2.6	136
26	Superior tensile properties of 1%C-CoCrFeMnNi high-entropy alloy additively manufactured by selective laser melting. Materials Research Letters, 2020, 8, 1-7.	4.1	135
27	Development of strong and ductile metastable face-centered cubic single-phase high-entropy alloys. Acta Materialia, 2019, 181, 318-330.	3.8	134
28	On the rule of mixtures for predicting the mechanical properties of composites with homogeneously distributed soft and hard particles. Journal of Materials Processing Technology, 2001, 112, 109-113.	3.1	130
29	Gas tungsten arc welding of as-rolled CrMnFeCoNi high entropy alloy. Materials and Design, 2020, 189, 108505.	3.3	125
30	High temperature oxidation behavior of Cr-Mn-Fe-Co-Ni high entropy alloy. Intermetallics, 2018, 98, 45-53.	1.8	120
31	Fabrication and mechanical properties of TiC reinforced CoCrFeMnNi high-entropy alloy composite by water atomization and spark plasma sintering. Journal of Alloys and Compounds, 2019, 781, 389-396.	2.8	120
32	Heterogeneous Aspects of Additive Manufactured Metallic Parts: A Review. Metals and Materials International, 2021, 27, 1-39.	1.8	119
33	Short-range order strengthening in boron-doped high-entropy alloys for cryogenic applications. Acta Materialia, 2020, 194, 366-377.	3.8	117
34	Ultrahigh high-strain-rate superplasticity in a nanostructured high-entropy alloy. Nature Communications, 2020, 11, 2736.	5.8	116
35	Dislocation density-based finite element analysis of large strain deformation behavior of copper under high-pressure torsion. Acta Materialia, 2014, 76, 281-293.	3.8	113
36	Finite element analysis of deformation behaviour of metals during equal channel multi-angular pressing. Materials Science & Engineering A: Structural Materials: Properties, Microstructure and Processing, 2002, 328, 317-323.	2.6	111

#	Article	IF	CITATIONS
37	Plastic Yield Behaviour of Porous Metals. Powder Metallurgy, 1992, 35, 275-280.	0.9	109
38	Phase mixture modeling of the strain rate dependent mechanical behavior of nanostructured materials. Acta Materialia, 2005, 53, 765-772.	3.8	108
39	Plastic deformation analysis of metals during equal channel angular pressing. Journal of Materials Processing Technology, 2001, 113, 622-626.	3.1	107
40	Enhanced plasticity in a bulk amorphous matrix composite: macroscopic and microscopic viewpoint studies. Acta Materialia, 2005, 53, 129-139.	3.8	102
41	Wear properties of ECAP-processed ultrafine grained Al–Cu alloys. Materials Science & Engineering A: Structural Materials: Properties, Microstructure and Processing, 2010, 527, 3726-3732.	2.6	102
42	Superior cryogenic tensile properties of ultrafine-grained CoCrNi medium-entropy alloy produced by high-pressure torsion and annealing. Scripta Materialia, 2019, 163, 152-156.	2.6	102
43	Mechanical properties and deformation twinning behavior of as-cast CoCrFeMnNi high-entropy alloy at low and high temperatures. Materials Science & Engineering A: Structural Materials: Properties, Microstructure and Processing, 2018, 712, 108-113.	2.6	98
44	Dissimilar laser welding of a CoCrFeMnNi high entropy alloy to 316 stainless steel. Scripta Materialia, 2022, 206, 114219.	2.6	98
45	Thermally activated deformation and the rate controlling mechanism in CoCrFeMnNi high entropy alloy. Materials Science & Engineering A: Structural Materials: Properties, Microstructure and Processing, 2017, 682, 569-576.	2.6	96
46	Development of TiNbTaZrMo bio-high entropy alloy (BioHEA) super-solid solution by selective laser melting, and its improved mechanical property and biocompatibility. Scripta Materialia, 2021, 194, 113658.	2.6	95
47	Review of principles and methods of severe plastic deformation for producing ultrafine-grained tubes. Materials Science and Technology, 2017, 33, 905-923.	0.8	93
48	Austenite stability and heterogeneous deformation in fine-grained transformation-induced plasticity-assisted steel. Scripta Materialia, 2013, 68, 933-936.	2.6	91
49	Effect of nanoparticle content on the microstructural and mechanical properties of nano-SiC dispersed bulk ultrafine-grained Cu matrix composites. Materials & Design, 2013, 52, 881-887.	5.1	91
50	Effects of strain hardenability and strain-rate sensitivity on the plastic flow and deformation homogeneity during equal channel angular pressing. Journal of Materials Research, 2001, 16, 856-864.	1.2	90
51	Deformation-induced nanocrystallization and its influence on work hardening in a bulk amorphous matrix composite. Acta Materialia, 2004, 52, 1525-1533.	3.8	90
52	Effect of μ-precipitates on the microstructure and mechanical properties of non-equiatomic CoCrFeNiMo medium-entropy alloys. Journal of Alloys and Compounds, 2019, 781, 75-83.	2.8	90
53	Deep learning-based phase prediction of high-entropy alloys: Optimization, generation, and explanation. Materials and Design, 2021, 197, 109260.	3.3	90
54	Ultra-high tensile strength nanocrystalline CoCrNi equi-atomic medium entropy alloy processed by high-pressure torsion. Materials Science & Engineering A: Structural Materials: Properties, Microstructure and Processing, 2018, 735, 394-397.	2.6	89

#	Article	IF	CITATIONS
55	Phosphorus doped ZnO light emitting diodes fabricated via pulsed laser deposition. Applied Physics Letters, 2008, 92, .	1.5	85
56	Trade-off between tensile property and formability by partial recrystallization of CrMnFeCoNi high-entropy alloy. Materials Science & Engineering A: Structural Materials: Properties, Microstructure and Processing, 2017, 703, 324-330.	2.6	85
57	Wear properties of high pressure torsion processed ultrafine grained Al–7%Si alloy. Materials & Design, 2014, 53, 373-382.	5.1	82
58	Surface Modification of Multipass Caliber-Rolled Ti Alloy with Dexamethasone-Loaded Graphene for Dental Applications. ACS Applied Materials & amp; Interfaces, 2015, 7, 9598-9607.	4.0	82
59	Improving the ductility in laser welded joints of CoCrFeMnNi high entropy alloy to 316 stainless steel. Materials and Design, 2022, 219, 110717.	3.3	81
60	Work-Hardening Induced Tensile Ductility of Bulk Metallic Glasses via High-Pressure Torsion. Scientific Reports, 2015, 5, 9660.	1.6	80
61	A new strategy for designing immiscible medium-entropy alloys with excellent tensile properties. Acta Materialia, 2020, 193, 71-82.	3.8	80
62	On the strain rate-dependent deformation mechanism of CoCrFeMnNi high-entropy alloy at liquid nitrogen temperature. Materials Research Letters, 2017, 5, 472-477.	4.1	78
63	Architecturing of Metalâ€Based Composites with Concurrent Nanostructuring: A New Paradigm of Materials Design. Advanced Engineering Materials, 2013, 15, 336-340.	1.6	76
64	Ultrastrong duplex high-entropy alloy with 2†GPa cryogenic strength enabled by an accelerated martensitic transformation. Scripta Materialia, 2019, 171, 67-72.	2.6	76
65	Annealing-induced hardening in high-pressure torsion processed CoCrNi medium entropy alloy. Materials Science & Engineering A: Structural Materials: Properties, Microstructure and Processing, 2018, 734, 338-340.	2.6	75
66	High-temperature tensile deformation behavior of hot rolled CrMnFeCoNi high-entropy alloy. Journal of Alloys and Compounds, 2018, 730, 242-248.	2.8	74
67	Finite element analysis of plastic deformation behavior during high pressure torsion processing. Journal of Materials Processing Technology, 2008, 201, 32-36.	3.1	73
68	Fabrication, characterization and mechanical properties of hybrid composites of copper using the nanoparticulates of SiC and carbon nanotubes. Materials Science & Engineering A: Structural Materials: Properties, Microstructure and Processing, 2013, 572, 83-90.	2.6	73
69	Effects of microstructure and internal defects on mechanical anisotropy and asymmetry of selective laser-melted 316L austenitic stainless steel. Materials Science & Engineering A: Structural Materials: Properties, Microstructure and Processing, 2019, 763, 138152.	2.6	73
70	Microstructure and hardness of copper–carbon nanotube composites consolidated by High Pressure Torsion. Materials Science & Engineering A: Structural Materials: Properties, Microstructure and Processing, 2011, 528, 4690-4695.	2.6	72
71	Consolidation of 1vol.% carbon nanotube reinforced metal matrix nanocomposites via equal channel angular pressing. Journal of Materials Processing Technology, 2007, 187-188, 318-320.	3.1	71
72	FCC to BCC transformation-induced plasticity based on thermodynamic phase stability in novel V10Cr10Fe45CoxNi35â^'x medium-entropy alloys. Scientific Reports, 2019, 9, 2948.	1.6	71

#	Article	IF	CITATIONS
73	A model of the ductile–brittle transition of partially crystallized amorphous Al–Ni–Y alloys. Acta Materialia, 1999, 47, 2059-2066.	3.8	70
74	Structural characterization of ultrafine-grained interstitial-free steel prepared by severe plastic deformation. Acta Materialia, 2016, 105, 258-272.	3.8	70
75	High-cycle fatigue and tensile deformation behaviors of coarse-grained equiatomic CoCrFeMnNi high entropy alloy and unexpected hardening behavior during cyclic loading. Intermetallics, 2019, 111, 106486.	1.8	70
76	Evaluation of Strain Rate During Equal-channel Angular Pressing. Journal of Materials Research, 2002, 17, 172-179.	1.2	69
77	Hygroscopic Auxetic On-Skin Sensors for Easy-to-Handle Repeated Daily Use. ACS Applied Materials & Interfaces, 2018, 10, 40141-40148.	4.0	69
78	A composite model for mechanical properties of nanocrystalline materials. Scripta Materialia, 1998, 39, 1057-1061.	2.6	68
79	Finite element analysis of equal channel angular pressing of strain rate sensitive metals. Journal of Materials Processing Technology, 2002, 130-131, 497-503.	3.1	68
80	Severe plastic deformation and strain localization in groove pressing. Computational Materials Science, 2008, 43, 641-645.	1.4	68
81	Microstructure inhomogeneity in ultra-fine grained bulk AZ91 produced by accumulative back extrusion (ABE). Materials Science & Engineering A: Structural Materials: Properties, Microstructure and Processing, 2011, 528, 4312-4317.	2.6	67
82	Unique microstructure and simultaneous enhancements of strength and ductility in gradient-microstructured Cu sheet produced by single-roll angular-rolling. Acta Materialia, 2019, 166, 638-649.	3.8	67
83	Utilization of brittle σ phase for strengthening and strain hardening in ductile VCrFeNi high-entropy alloy. Materials Science & Engineering A: Structural Materials: Properties, Microstructure and Processing, 2019, 743, 665-674.	2.6	67
84	A perspective on precipitation-hardening high-entropy alloys fabricated by additive manufacturing. Materials and Design, 2021, 211, 110161.	3.3	67
85	Correlation between fracture toughness and stretch-flangeability of advanced high strength steels. Materials Letters, 2016, 180, 322-326.	1.3	66
86	Wear and friction behavior of self-lubricating hybrid Cu-(SiC + x CNT) composites. Composites Part B: Engineering, 2019, 158, 92-101.	5.9	66
87	Towards ferrous medium-entropy alloys with low-cost and high-performance. Scripta Materialia, 2020, 186, 169-173.	2.6	66
88	Effect of the gap distance on the cooling behavior and the microstructure of indirect squeeze cast and gravity die cast 5083 wrought Al alloy. Materials Science & Engineering A: Structural Materials: Properties, Microstructure and Processing, 2002, 338, 182-190.	2.6	65
89	Finite element analysis of high pressure torsion processing. Journal of Materials Processing Technology, 2001, 113, 617-621.	3.1	64
90	Microstructural features, texture and strengthening mechanisms of nanostructured AA6063 alloy processed by powder metallurgy. Materials Science & Engineering A: Structural Materials: Properties, Microstructure and Processing, 2011, 528, 3981-3989.	2.6	64

#	Article	IF	CITATIONS
91	Finite element analysis of plastic deformation in twist extrusion. Computational Materials Science, 2012, 60, 194-200.	1.4	64
92	Space-holder effect on designing pore structure and determining mechanical properties in porous titanium. Materials & Design, 2014, 57, 712-718.	5.1	64
93	Evolution of microstructure and hardness in AZ31 alloy processed by high pressure torsion. Materials Science & Engineering A: Structural Materials: Properties, Microstructure and Processing, 2015, 625, 98-106.	2.6	64
94	Twist Extrusion as a Potent Tool for Obtaining Advanced Engineering Materials: A Review. Advanced Engineering Materials, 2017, 19, 1600873.	1.6	64
95	Metalloid substitution elevates simultaneously the strength and ductility of face-centered-cubic high-entropy alloys. Acta Materialia, 2022, 225, 117571.	3.8	64
96	Plastic flow and deformation homogeneity of 6061 Al during equal channel angular pressing. Scripta Materialia, 2002, 46, 131-136.	2.6	63
97	3D FEM simulations for the homogeneity of plastic deformation in Al–Cu alloys during ECAP. Materials Science & Engineering A: Structural Materials: Properties, Microstructure and Processing, 2010, 527, 1404-1410.	2.6	62
98	High temperature thermal stability of pure copper and copper–carbon nanotube composites consolidated by High Pressure Torsion. Composites Part A: Applied Science and Manufacturing, 2013, 51, 71-79.	3.8	62
99	An efficient machine learning approach to establish structure-property linkages. Computational Materials Science, 2019, 156, 17-25.	1.4	62
100	Effect of Equal Channel Angular Pressing on Microstructure and Mechanical Properties of IF Steel. Advanced Engineering Materials, 2005, 7, 43-46.	1.6	61
101	Method for measuring nanoscale local strain in a dual phase steel using digital image correlation with nanodot patterns. Scripta Materialia, 2013, 68, 245-248.	2.6	61
102	Effect of annealing heat treatment on microstructural evolution and tensile behavior of Al0.5CoCrFeMnNi high-entropy alloy. Materials Science & Engineering A: Structural Materials: Properties, Microstructure and Processing, 2018, 728, 251-258.	2.6	61
103	Beating Thermal Coarsening in Nanoporous Materials via Highâ€Entropy Design. Advanced Materials, 2020, 32, e1906160.	11.1	61
104	Effects of residual stress on the mechanical properties of copper processed using ultrasonic-nanocrystalline surface modification. Materials Research Letters, 2019, 7, 97-102.	4.1	60
105	Ductility of ultrafine grained copper. Applied Physics Letters, 2001, 79, 4115-4117.	1.5	59
106	Compressive deformation behavior of CrMnFeCoNi high-entropy alloy. Metals and Materials International, 2016, 22, 982-986.	1.8	59
107	Quasi-static and dynamic deformation mechanisms interpreted by microstructural evolution in TWinning Induced Plasticity (TWIP) steel. Materials Science & Engineering A: Structural Materials: Properties, Microstructure and Processing, 2017, 684, 54-63.	2.6	59
108	Role of BCC phase on tensile behavior of dual-phase Al0.5CoCrFeMnNi high-entropy alloy at cryogenic temperature. Materials Science & amp; Engineering A: Structural Materials: Properties, Microstructure and Processing, 2019, 746, 443-447.	2.6	59

#	Article	IF	CITATIONS
109	Precipitation-driven metastability engineering of carbon-doped CoCrFeNiMo medium-entropy alloys at cryogenic temperature. Scripta Materialia, 2020, 188, 140-145.	2.6	59
110	Laser weldability of cast and rolled high-entropy alloys for cryogenic applications. Materials Science & Engineering A: Structural Materials: Properties, Microstructure and Processing, 2019, 742, 224-230.	2.6	59
111	High tensile ductility of Ti-based amorphous matrix composites modified from conventional Ti–6Al–4V titanium alloy. Acta Materialia, 2013, 61, 3012-3026.	3.8	58
112	Nano-scale heterogeneity-driven metastability engineering in ferrous medium-entropy alloy induced by additive manufacturing. Acta Materialia, 2021, 221, 117426.	3.8	58
113	Microstructural development and mechanical properties of nanostructured copper reinforced with SiC nanoparticles. Materials Science & Engineering A: Structural Materials: Properties, Microstructure and Processing, 2013, 568, 33-39.	2.6	57
114	Effect of post weld heat treatment on weldability of high entropy alloy welds. Science and Technology of Welding and Joining, 2018, 23, 420-427.	1.5	57
115	Cryogenic-temperature fracture toughness analysis of non-equi-atomic V10Cr10Fe45Co20Ni15 high-entropy alloy. Journal of Alloys and Compounds, 2019, 809, 151864.	2.8	57
116	Constitutive modelling of strength and plasticity of nanocrystalline metallic materials. Materials Science & Engineering A: Structural Materials: Properties, Microstructure and Processing, 2001, 316, 195-199.	2.6	56
117	Effect of strain rate on compressive behavior of Ti45Zr16Ni9Cu10Be20 bulk metallic glass. Materials Science & Engineering A: Structural Materials: Properties, Microstructure and Processing, 2007, 449-451, 290-294.	2.6	56
118	Mechanical properties of copper after compression stage of high-pressure torsion. Materials Science & Engineering A: Structural Materials: Properties, Microstructure and Processing, 2011, 528, 4840-4844.	2.6	56
119	Mechanical properties and microstructural evaluation of AA1100 to AZ31 dissimilar friction stir welds. Materials Chemistry and Physics, 2016, 170, 251-260.	2.0	56
120	The dead metal zone in high-pressure torsion. Scripta Materialia, 2012, 67, 384-387.	2.6	55
121	Deformation-induced phase transformation of Co20Cr26Fe20Mn20Ni14 high-entropy alloy during high-pressure torsion at 77 K. Materials Letters, 2017, 202, 86-88.	1.3	55
122	Wear properties of brass samples subjected to constrained groove pressing process. Materials & Design, 2014, 63, 531-537.	5.1	54
123	Mechanical, tribological and electrical properties of Cu-CNT composites fabricated by flake powder metallurgy method. Archives of Civil and Mechanical Engineering, 2019, 19, 694-706.	1.9	54
124	Microstructural evolution of liquid metal embrittlement in resistance-spot-welded galvanized TWinning-Induced Plasticity (TWIP) steel sheets. Materials Characterization, 2019, 147, 233-241.	1.9	54
125	In-situ carbide-reinforced CoCrFeMnNi high-entropy alloy matrix nanocomposites manufactured by selective laser melting: Carbon content effects on microstructure, mechanical properties, and deformation mechanism. Composites Part B: Engineering, 2021, 210, 108638.	5.9	54
126	A phase mixture model of a particle reinforced composite with fine microstructure. Materials Science & Engineering A: Structural Materials: Properties, Microstructure and Processing, 2000, 276, 175-185.	2.6	53

#	Article	IF	CITATIONS
127	Twinning Engineering of a CoCrFeMnNi High-Entropy Alloy. Scripta Materialia, 2021, 197, 113808.	2.6	53
128	Numerical and experimental investigation of the deformation behavior during the accumulative back extrusion of an AZ91 magnesium alloy. Materials & Design, 2012, 35, 251-258.	5.1	52
129	Mechanical behavior and solid solution strengthening model for face-centered cubic single crystalline and polycrystalline high-entropy alloys. Intermetallics, 2018, 98, 89-94.	1.8	52
130	Dynamic strain aging of twinning-induced plasticity (TWIP) steel in tensile testing and deep drawing. Materials Science & Engineering A: Structural Materials: Properties, Microstructure and Processing, 2015, 633, 136-143.	2.6	51
131	Factors governing hole expansion ratio of steel sheets with smooth sheared edge. Metals and Materials International, 2016, 22, 1009-1014.	1.8	51
132	Effect of grain size on the tensile behavior of V10Cr15Mn5Fe35Co10Ni25 high entropy alloy. Materials Science & Engineering A: Structural Materials: Properties, Microstructure and Processing, 2019, 744, 610-617.	2.6	51
133	Deformation behavior of a Co-Cr-Fe-Ni-Mo medium-entropy alloy at extremely low temperatures. Materials Today, 2021, 50, 55-68.	8.3	51
134	Mechanical properties of partially crystallized aluminum based amorphous alloys. Scripta Materialia, 1999, 11, 241-247.	0.5	50
135	Heavily drawn Cu–Fe–Ag and Cu–Fe–Cr microcomposites. Journal of Materials Processing Technology, 2001, 113, 610-616.	3.1	50
136	Microstructure and compressibility of SiC nanoparticles reinforced Cu nanocomposite powders processed by high energy mechanical milling. Ceramics International, 2014, 40, 951-960.	2.3	50
137	Effects of (W, Cr) carbide on grain refinement and mechanical properties for CoCrFeMnNi high entropy alloys. Journal of Alloys and Compounds, 2019, 770, 222-228.	2.8	50
138	Exceptional cryogenic strength-ductility synergy in Al0.3CoCrNi medium-entropy alloy through heterogeneous grain structure and nano-scale precipitates. Materials Science & Engineering A: Structural Materials: Properties, Microstructure and Processing, 2019, 766, 138372.	2.6	50
139	Nano-scale solute heterogeneities in the ultrastrong selectively laser melted carbon-doped CoCrFeMnNi alloy. Materials Science & Engineering A: Structural Materials: Properties, Microstructure and Processing, 2020, 773, 138726.	2.6	50
140	A powder-metallurgy-based fabrication route towards achieving high tensile strength with ultra-high ductility in high-entropy alloy. Scripta Materialia, 2021, 190, 69-74.	2.6	50
141	Die design for homogeneous plastic deformation during equal channel angular pressing. Journal of Materials Processing Technology, 2007, 187-188, 46-50.	3.1	49
142	Role of brittle sigma phase in cryogenic-temperature-strength improvement of non-equi-atomic Fe-rich VCrMnFeCoNi high entropy alloys. Materials Science & Engineering A: Structural Materials: Properties, Microstructure and Processing, 2018, 724, 403-410.	2.6	49
143	Fine tuning of tensile properties in CrCoNi medium entropy alloy through cold rolling and annealing. Intermetallics, 2019, 113, 106578.	1.8	49
144	Microstructural modelling of equal channel angular pressing for producing ultrafine grained materials. Materials Science & Engineering A: Structural Materials: Properties, Microstructure and Processing, 2005, 410-411, 285-289.	2.6	48

#	Article	IF	CITATIONS
145	Constitutive modeling of deformation behavior of high-entropy alloys with face-centered cubic crystal structure. Materials Research Letters, 2017, 5, 350-356.	4.1	48
146	Novel 1.5 GPa-strength with 50%-ductility by transformation-induced plasticity of non-recrystallized austenite in duplex steels. Scientific Reports, 2017, 7, 1255.	1.6	48
147	Superior Strength and Multiple Strengthening Mechanisms in Nanocrystalline TWIP Steel. Scientific Reports, 2018, 8, 11200.	1.6	48
148	Strength enhancement of high entropy alloy HfNbTaTiZr by severe plastic deformation. Journal of Alloys and Compounds, 2018, 768, 924-937.	2.8	48
149	High-Output and Bending-Tolerant Triboelectric Nanogenerator Based on an Interlocked Array of Surface-Functionalized Indium Tin Oxide Nanohelixes. ACS Energy Letters, 2019, 4, 1748-1754.	8.8	48
150	Evidence of FCC to HCP and BCC-martensitic transformations in a CoCrFeNiMn high-entropy alloy by severe plastic deformation. Materials Science & Engineering A: Structural Materials: Properties, Microstructure and Processing, 2021, 807, 140875.	2.6	48
151	Achieving high strength and high ductility in Al0.3CoCrNi medium-entropy alloy through multi-phase hierarchical microstructure. Materialia, 2019, 8, 100442.	1.3	47
152	Calculation of Deformation Behavior and Texture Evolution during Equal Channel Angular Pressing of IF Steel Using Dislocation Based Modeling of Strain Hardening. Materials Science Forum, 2002, 408-412, 697-702.	0.3	46
153	Deformation behavior of copper during a high pressure torsion process. Journal of Materials Processing Technology, 2003, 142, 334-337.	3.1	46
154	A comment on the role of Frank–Read sources in plasticity of nanomaterials. Acta Materialia, 2007, 55, 6401-6407.	3.8	46
155	Microstructure and mechanical properties of a Mg–Zn–Y alloy produced by a powder metallurgy route. Journal of Alloys and Compounds, 2014, 586, S95-S100.	2.8	46
156	Shape memory effect in nanocrystalline NiTi alloy processed by high-pressure torsion. Materials Science & Engineering A: Structural Materials: Properties, Microstructure and Processing, 2015, 626, 203-206.	2.6	46
157	Effects of deformation–induced BCC martensitic transformation and twinning on impact toughness and dynamic tensile response in metastable VCrFeCoNi high–entropy alloy. Journal of Alloys and Compounds, 2019, 785, 1056-1067.	2.8	46
158	Plastic Deformation Behavior of 40Fe–25Ni–15Cr–10Co–10V High-Entropy Alloy for Cryogenic Applications. Metals and Materials International, 2019, 25, 277-284.	1.8	46
159	Enhanced tensile properties and electrical conductivity of Cu-CNT nanocomposites processed via the combination of flake powder metallurgy and high pressure torsion methods. Materials Science & Engineering A: Structural Materials: Properties, Microstructure and Processing, 2020, 773, 138888.	2.6	46
160	Influence of nanoprecipitation on strength of Cu60Zr30Ti10 glass containing μm-ZrC particle reinforcements. Scripta Materialia, 2004, 51, 577-581.	2.6	45
161	Microstructure, texture and mechanical properties of the magnesium alloy AZ31 processed by ECAP. International Journal of Materials Research, 2008, 99, 50-55.	0.1	45
162	Effects of the spin line temperature profile and melt index of poly(propylene) on meltâ€electrospinning. Polymer Engineering and Science, 2009, 49, 391-396.	1.5	45

#	Article	IF	CITATIONS
163	Grain refinement under high strain rate impact: A numerical approach. Computational Materials Science, 2010, 48, 124-132.	1.4	45
164	A combination of severe plastic deformation and ageing phenomena in Al–Mg–Si Alloys. Materials & Design, 2012, 36, 735-740.	5.1	45
165	Microstructure, plastic deformation and strengthening mechanisms of an Al–Mg–Si alloy with a bimodal grain structure. Journal of Alloys and Compounds, 2015, 632, 540-548.	2.8	45
166	Microstructure and Mechanical Properties of High-Entropy Alloy Co20Cr26Fe20Mn20Ni14 Processed by High-Pressure Torsion at 77 K and 300 K. Scientific Reports, 2018, 8, 11074.	1.6	45
167	Modeling of texture evolution in copper under equal channel angular pressing. International Journal of Materials Research, 2003, 94, 1189-1198.	0.8	44
168	Nano-web formation by the electrospinning at various electric fields. Journal of Materials Science, 2007, 42, 8106-8112.	1.7	44
169	Microstructure and tensile behavior of Al and Al-matrix carbon nanotube composites processed by high pressure torsion of the powders. Journal of Materials Science, 2010, 45, 4652-4658.	1.7	44
170	Effect of high-pressure torsion on the microstructure and strengthening mechanisms of hot-consolidated Cu–CNT nanocomposite. Materials Science & Engineering A: Structural Materials: Properties, Microstructure and Processing, 2015, 638, 289-295.	2.6	44
171	Suppressed deformation instability in the twinning-induced plasticity steel-cored three-layer steel sheet. Acta Materialia, 2018, 147, 304-312.	3.8	44
172	Microstructural behavior of rapidly solidified and extruded Al-14wt%Ni-14wt%Mm (Mm, misch metal) alloy powders. Materials Science & Engineering A: Structural Materials: Properties, Microstructure and Processing, 1999, 271, 469-476.	2.6	43
173	Effects of microstructure and yield ratio on strain hardening and Bauschinger effect in two API X80 linepipe steels. Materials Science & Engineering A: Structural Materials: Properties, Microstructure and Processing, 2012, 551, 192-199.	2.6	43
174	Toward excellent tensile properties of nitrogen-doped CoCrFeMnNi high-entropy alloy at room and cryogenic temperatures. Journal of Alloys and Compounds, 2022, 897, 163217.	2.8	43
175	Finite element analysis of the effect of the inner corner angle in equal channel angular pressing. Materials Science & Engineering A: Structural Materials: Properties, Microstructure and Processing, 2008, 490, 438-444.	2.6	41
176	Dynamic ageing and the mechanical response of Al–Mg–Si alloy through equal channel angular pressing. Materials & Design, 2010, 31, 4076-4082.	5.1	41
177	Grain refinement and tensile strength of carbon nanotube-reinforced Cu matrix nanocomposites processed by high-pressure torsion. Metals and Materials International, 2013, 19, 927-932.	1.8	41
178	Effects of transformation-induced plasticity (TRIP) on tensile property improvement of Fe45Co30Cr10V10Ni5-xMnx high-entropy alloys. Materials Science & Engineering A: Structural Materials: Properties, Microstructure and Processing, 2020, 772, 138809.	2.6	41
179	Analysis of damage-tolerance of TRIP-assisted V10Cr10Fe45Co30Ni5 high-entropy alloy at room and cryogenic temperatures. Journal of Alloys and Compounds, 2020, 844, 156090.	2.8	41
180	Worn surface and subsurface layer structure formation behavior on wear mechanism of CoCrFeMnNi high entropy alloy in different sliding conditions. Applied Surface Science, 2021, 549, 149202.	3.1	41

#	Article	IF	CITATIONS
181	Numerical Investigation of Mechanical Behaviour of Nanocrystalline Copper. Powder Metallurgy, 1998, 41, 217-220.	0.9	40
182	Dielectric passivation effects on ZnO light emitting diodes. Applied Physics Letters, 2008, 92, .	1.5	40
183	An experimental verification of the finite element modelling of equal channel angular pressing. Computational Materials Science, 2009, 46, 347-351.	1.4	40
184	Serration Phenomena Occurring During Tensile Tests of Three High-Manganese Twinning-Induced Plasticity (TWIP) Steels. Metallurgical and Materials Transactions A: Physical Metallurgy and Materials Science, 2014, 45, 633-646.	1.1	40
185	Deformation rate controls atomic-scale dynamic strain aging and phase transformation in high Mn TRIP steels. Acta Materialia, 2017, 131, 187-196.	3.8	40
186	Effect of Annealing on Microstructure and Tensile Behavior of CoCrNi Medium Entropy Alloy Processed by High-Pressure Torsion. Entropy, 2018, 20, 849.	1.1	40
187	Band-edge electroluminescence from N+-implanted bulk ZnO. Applied Physics Letters, 2006, 88, 102107.	1.5	39
188	Consolidation of Carbon Nanotube Reinforced Aluminum Matrix Composites by High-Pressure Torsion. Metallurgical and Materials Transactions A: Physical Metallurgy and Materials Science, 2014, 45, 4129-4137.	1.1	39
189	Strain-rate sensitivity of high-entropy alloys and its significance in deformation. Materials Research Letters, 2019, 7, 503-509.	4.1	39
190	Low-cycle fatigue properties of CoCrFeMnNi high-entropy alloy compared with its conventional counterparts. Materials Science & Engineering A: Structural Materials: Properties, Microstructure and Processing, 2020, 792, 139661.	2.6	39
191	Processing and microstructure of Ti-Cu binary alloys: A comprehensive review. Progress in Materials Science, 2022, 127, 100933.	16.0	39
192	Elastoplastic Finite Element Analysis for Porous Metals. Powder Metallurgy, 1994, 37, 140-146.	0.9	38
193	Modelling microstructure evolution toward ultrafine crystallinity produced by severe plastic deformation. Journal of Materials Science, 2007, 42, 1512-1516.	1.7	38
194	Key factors of stretch-flangeability of sheet materials. Journal of Materials Science, 2017, 52, 7808-7823.	1.7	38
195	Fine-tuning of mechanical properties in V10Cr15Mn5Fe35Co10Ni25 high-entropy alloy through high-pressure torsion and annealing. Materials Science & Engineering A: Structural Materials: Properties, Microstructure and Processing, 2020, 771, 138604.	2.6	38
196	Breaking the limit of Young's modulus in low-cost Ti–Nb–Zr alloy for biomedical implant applications. Journal of Alloys and Compounds, 2020, 828, 154401.	2.8	38
197	Ultra-strong and strain-hardenable ultrafine-grained medium-entropy alloy via enhanced grain-boundary strengthening. Materials Research Letters, 2021, 9, 315-321.	4.1	38
198	Finite element analysis of the plastic deformation in tandem process of simple shear extrusion and twist extrusion. Materials and Design, 2015, 83, 858-865.	3.3	37

#	Article	IF	CITATIONS
199	Laser dissimilar weldability of cast and rolled CoCrFeMnNi high-entropy alloys for cryogenic applications. Science and Technology of Welding and Joining, 2020, 25, 127-134.	1.5	37
200	Effects of annealing temperature on microstructures and tensile properties of a single FCC phase CoCuMnNi high-entropy alloy. Journal of Alloys and Compounds, 2020, 812, 152111.	2.8	37
201	Exploration of optimal microstructure and mechanical properties in continuous microstructure space using a variational autoencoder. Materials and Design, 2021, 202, 109544.	3.3	37
202	Hardening behaviour of partially crystallised amorphous Al alloys. Materials Science & Engineering A: Structural Materials: Properties, Microstructure and Processing, 2001, 304-306, 327-331.	2.6	36
203	Effects of Aluminum Addition on Tensile and Cup Forming Properties of Three Twinning Induced Plasticity Steels. Metallurgical and Materials Transactions A: Physical Metallurgy and Materials Science, 2012, 43, 1870-1883.	1.1	36
204	Effects of intergranular carbide precipitation on delayed fracture behavior in three TWinning Induced Plasticity (TWIP) steels. Materials Science & Engineering A: Structural Materials: Properties, Microstructure and Processing, 2013, 587, 85-99.	2.6	36
205	A Highly Sensitive Force Sensor with Fast Response Based on Interlocked Arrays of Indium Tin Oxide Nanosprings toward Human Tactile Perception. Advanced Functional Materials, 2018, 28, 1804132.	7.8	36
206	Back-Stress Effect on the Mechanical Strength of TWIP-IF Steels Layered Sheet. Metals and Materials International, 2019, 25, 912-917.	1.8	36
207	Enhanced cryogenic tensile properties with multi-stage strain hardening through partial recrystallization in a ferrous medium-entropy alloy. Scripta Materialia, 2021, 194, 113653.	2.6	36
208	Surfaceâ€Tailored Medium Entropy Alloys as Radically Low Overpotential Oxygen Evolution Electrocatalysts. Small, 2022, 18, e2105611.	5.2	36
209	Recycling of AlSi8Cu3 alloy chips via high pressure torsion. Materials Science & Engineering A: Structural Materials: Properties, Microstructure and Processing, 2013, 560, 121-128.	2.6	35
210	Cross Flow During Twist Extrusion: Theory, Experiment, and Application. Metallurgical and Materials Transactions A: Physical Metallurgy and Materials Science, 2013, 44, 3211-3220.	1.1	35
211	Microstructure, strengthening mechanisms and hot deformation behavior of an oxide-dispersion strengthened UFG Al6063 alloy. Materials Characterization, 2013, 75, 108-114.	1.9	35
212	Crystal plasticity modeling of the effect of precipitate states on the work hardening and plastic anisotropy in an Al–Mg–Si alloy. Computational Materials Science, 2014, 83, 78-85.	1.4	35
213	Cyclic Loading Test for Beam-Column Connections of Concrete-Filled U-Shaped Steel Beams and Concrete-Encased Steel Angle Columns. Journal of Structural Engineering, 2015, 141, .	1.7	35
214	Dynamic tension–compression asymmetry of martensitic transformation in austenitic Fe–(0.4,) Tj ETQq0 0 () rgBT /Ov	erlggk 10 Tf 5
215	Development of an oxide-dispersion-strengthened steel by introducing oxygen carrier compound into the melt aided by a general thermodynamic model. Scientific Reports, 2016, 6, 38621.	1.6	35

216Modelling of the Evolution of Dislocation Cell Misorientation under Severe Plastic Deformation.0.334216Materials Science Forum, 2006, 503-504, 675-680.0.334

#	Article	IF	CITATIONS
217	Tensile properties and fracture characteristics of ECAP-processed Al and Al-Cu alloys. Metals and Materials International, 2010, 16, 709-716.	1.8	34
218	Microstructure and Mechanical Properties of Oxide-Dispersion Strengthened Al6063 Alloy with Ultra-Fine Grain Structure. Metallurgical and Materials Transactions A: Physical Metallurgy and Materials Science, 2011, 42, 816-824.	1.1	34
219	Real Hydrostatic Pressure in High-Pressure Torsion Measured by Bismuth Phase Transformations and FEM Simulations. Materials Transactions, 2016, 57, 533-538.	0.4	34
220	Multiscale architectured materials with composition and grain size gradients manufactured using high-pressure torsion. Scientific Reports, 2016, 6, 26590.	1.6	34
221	Fabrication of Al/Al 2 Cu in situ nanocomposite via friction stir processing. Transactions of Nonferrous Metals Society of China, 2017, 27, 779-788.	1.7	34
222	Understanding of adiabatic shear band evolution during high-strain-rate deformation in high-strength armor steel. Journal of Alloys and Compounds, 2020, 845, 155540.	2.8	34
223	Hetero-deformation-induced strengthening by twin-mediated martensitic transformation in an immiscible medium-entropy alloy. Scripta Materialia, 2020, 186, 24-28.	2.6	34
224	Obtaining Reliable True Plastic Stress-Strain Curves in a Wide Range of Strains Using Digital Image Correlation in Tensile Testing. Journal of Korean Institute of Metals and Materials, 2016, 54, 231-236.	0.4	34
225	A constitutive model for densification of metal compacts: the case of copper. Materials Science & Engineering A: Structural Materials: Properties, Microstructure and Processing, 2001, 307, 67-73.	2.6	33
226	Preform effect on the plastic deformation behavior of workpieces in equal channel angular pressing. Scripta Materialia, 2006, 55, 159-162.	2.6	33
227	Microstructural Evolution of UFG Magnesium Alloy Produced by Accumulative Back Extrusion (ABE). Materials and Manufacturing Processes, 2012, 27, 267-272.	2.7	33
228	Effect of starting materials on the wear performance of NiTi-based composites. Wear, 2015, 334-335, 35-43.	1.5	33
229	Shock wave compaction and sintering of mechanically alloyed CoCrFeMnNi high-entropy alloy powders. Materials Science & Engineering A: Structural Materials: Properties, Microstructure and Processing, 2017, 708, 291-300.	2.6	33
230	Single-roll angular-rolling: A new continuous severe plastic deformation process for metal sheets. Scripta Materialia, 2018, 146, 204-207.	2.6	33
231	Relationships Between Stretch-Flangeability and Microstructure-Mechanical Properties in Ultra-High-Strength Dual-Phase Steels. Metals and Materials International, 2019, 25, 1161-1169.	1.8	33
232	Effects of Cell Network Structure on the Strength of Additively Manufactured Stainless Steels. Metals and Materials International, 2021, 27, 2614-2622.	1.8	33
233	Yield and compaction behavior of rapidly solidified Al–Si alloy powders. Materials Science & Engineering A: Structural Materials: Properties, Microstructure and Processing, 1998, 251, 100-105.	2.6	32
234	Effect of nano Al2O3 addition on mechanical properties and wear behavior of NiTi intermetallic. Materials & Design, 2013, 51, 375-382.	5.1	32

#	Article	IF	CITATIONS
235	Interfacial microstructures and properties of aluminum alloys/galvanized low-carbon steel under high-pressure torsion. Materials & Design, 2014, 64, 287-293.	5.1	32
236	Continuum understanding of twin formation near grain boundaries of FCC metals with low stacking fault energy. Npj Computational Materials, 2017, 3, .	3.5	32
237	Effect of secondary phase particles on the tensile behavior of Mg-Zn-Ca alloy. Materials Science & Engineering A: Structural Materials: Properties, Microstructure and Processing, 2018, 735, 288-294.	2.6	32
238	Bayesian approach in predicting mechanical properties of materials: Application to dual phase steels. Materials Science & Engineering A: Structural Materials: Properties, Microstructure and Processing, 2019, 743, 382-390.	2.6	32
239	Isotropic and kinematic hardening of a high entropy alloy. Scripta Materialia, 2021, 191, 107-110.	2.6	32
240	Deformation-induced grain boundary segregation mediated high-strain rate superplasticity in medium entropy alloy. Scripta Materialia, 2022, 207, 114239.	2.6	32
241	Deformation Behavior in Tubular Channel Angular Pressing (TCAP) Using Triangular and Semicircular Channels. Materials Transactions, 2012, 53, 8-12.	0.4	31
242	Microstructures and mechanical properties of Mg–Zn–Y alloy consolidated from gas-atomized powders using high-pressure torsion. Journal of Materials Science, 2012, 47, 7117-7123.	1.7	31
243	Dynamic restoration and microstructural evolution during hot deformation of a P/M Al6063 alloy. Materials Science & Engineering A: Structural Materials: Properties, Microstructure and Processing, 2012, 542, 56-63.	2.6	31
244	Annealing behavior and shape memory effect in NiTi alloy processed by equal-channel angular pressing at room temperature. Materials Science & Engineering A: Structural Materials: Properties, Microstructure and Processing, 2015, 629, 16-22.	2.6	31
245	Microstructural evolution and strain-hardening behavior of multi-pass caliber-rolled Ti–13Nb–13Zr. Materials Science & Engineering A: Structural Materials: Properties, Microstructure and Processing, 2015, 648, 359-366.	2.6	31
246	Deformation processing and mechanical properties of Cu–Cr–X (X=Ag or Co) microcomposites. Journal of Materials Processing Technology, 2002, 130-131, 272-277.	3.1	30
247	Kinetic dislocation model of microstructure evolution during severe plastic deformation. Materials Science & Engineering A: Structural Materials: Properties, Microstructure and Processing, 2007, 460-461, 619-623.	2.6	30
248	Ton-scale metal–carbon nanotube composite: The mechanism of strengthening while retaining tensile ductility. Extreme Mechanics Letters, 2016, 8, 245-250.	2.0	30
249	Fabrication of NiTi and NiTi-nano Al2O3 composites by powder metallurgy methods: Comparison of hot isostatic pressing and spark plasma sintering techniques. Ceramics International, 2018, 44, 15981-15988.	2.3	30
250	Hardness, wear and friction characteristics of nanostructured Cu-SiC nanocomposites fabricated by powder metallurgy route. Materials Today Communications, 2019, 18, 25-31.	0.9	30
251	Effect of Initial Grain Size on Friction Stir Weldability for Rolled and Cast CoCrFeMnNi High-Entropy Alloys. Metals and Materials International, 2020, 26, 641-649.	1.8	30
252	Constitutive Modeling with Critical Twinning Stress in CoCrFeMnNi High Entropy Alloy at Cryogenic Temperature and Room Temperature. Metals and Materials International, 2021, 27, 2300-2309.	1.8	30

#	Article	IF	CITATIONS
253	Effect of die geometry on the microstructure of indirect squeeze cast and gravity die cast 5083 wrought Al alloy and numerical analysis of the cooling behavior. Journal of Materials Processing Technology, 1999, 96, 188-197.	3.1	29
254	Shear banding behavior and fracture mechanisms of Zr55Al10Ni5Cu30 bulk metallic glass in uniaxial compression analyzed using a digital image correlation method. Intermetallics, 2013, 32, 21-29.	1.8	29
255	Wear Behavior of AZ31/Al2O3 Magnesium Matrix Surface Nanocomposite Fabricated via Friction Stir Processing. Journal of Materials Engineering and Performance, 2018, 27, 2010-2017.	1.2	29
256	Fundamentals of Severe Plastic Deformation. , 2018, , 19-36.		29
257	Microstructural Evolution and Mechanical Properties in Superlight Mg-Li Alloy Processed by High-Pressure Torsion. Materials, 2018, 11, 598.	1.3	29
258	Weldability of cast CoCrFeMnNi high-entropy alloys using various filler metals for cryogenic applications. Journal of Alloys and Compounds, 2020, 819, 153278.	2.8	29
259	Microstructure design using machine learning generated low dimensional and continuous design space. Materialia, 2020, 11, 100690.	1.3	29
260	Plastic deformation characteristics of cross-equal channel angular pressing. Computational Materials Science, 2008, 43, 1069-1073.	1.4	28
261	Microstructural characterization of HIP consolidated NiTi–nano Al2O3 composites. Journal of Alloys and Compounds, 2014, 606, 21-26.	2.8	28
262	Outstanding mechanical properties of high-pressure torsion processed multiscale TWIP-cored three layer steel sheet. Scripta Materialia, 2016, 123, 122-125.	2.6	28
263	Synergistic role of carbon nanotube and SiCn reinforcements on mechanical properties and corrosion behavior of Cu-based nanocomposite developed by flake powder metallurgy and spark plasma sintering process. Materials Science & amp; Engineering A: Structural Materials: Properties, Microstructure and Processing, 2020, 786, 139395.	2.6	28
264	Architectured multi-metal CoCrFeMnNi-Inconel 718 lamellar composite by high-pressure torsion. Scripta Materialia, 2021, 195, 113722.	2.6	28
265	Simultaneous effects of deformation-induced plasticity and precipitation hardening in metastable non-equiatomic FeNiCoMnTiSi ferrous medium-entropy alloy at room and liquid nitrogen temperatures. Scripta Materialia, 2021, 202, 114013.	2.6	28
266	Microstructure, grain growth, and hardness during annealing of nanocrystalline Cu powders synthesized via high energy mechanical milling. Materials and Design, 2015, 83, 644-650.	3.3	27
267	Microstructure evolution and mechanical properties of pure aluminum deformed by equal channel angular pressing and direct extrusion in one step through an integrated die. Materials Science & Engineering A: Structural Materials: Properties, Microstructure and Processing, 2015, 625, 252-263.	2.6	27
268	Structural and phase transformation in a TWIP steel subjected to high pressure torsion. Materials Letters, 2016, 166, 321-324.	1.3	27
269	Tensile property improvement of TWIP-cored three-layer steel sheets fabricated by hot-roll-bonding with low-carbon steel or interstitial-free steel. Scientific Reports, 2017, 7, 40231.	1.6	27
270	Superior Pre-Osteoblast Cell Response of Etched Ultrafine-Grained Titanium with a Controlled Crystallographic Orientation. Scientific Reports, 2017, 7, 44213.	1.6	27

#	Article	IF	CITATIONS
271	Interpretation of quasi-static and dynamic tensile behavior by digital image correlation technique in TWinning Induced Plasticity (TWIP) and low-carbon steel sheets. Materials Science & Engineering A: Structural Materials: Properties, Microstructure and Processing, 2017, 693, 170-177.	2.6	27
272	Three-dimensional microstructure modeling of particulate composites using statistical synthetic structure and its thermo-mechanical finite element analysis. Computational Materials Science, 2017, 126, 265-271.	1.4	27
273	In situ neutron diffraction study of phase stress evolution in a ferrous medium-entropy alloy under low-temperature tensile loading. Scripta Materialia, 2019, 165, 60-63.	2.6	27
274	Strength and ductility enhancement in the gradient structured twinning-induced plasticity steel by ultrasonic nanocrystalline surface modification. Materials Science & Engineering A: Structural Materials: Properties, Microstructure and Processing, 2019, 739, 105-108.	2.6	27
275	Effect of grain size on the low-cycle fatigue behavior of carbon-containing high-entropy alloys. Materials Science & Engineering A: Structural Materials: Properties, Microstructure and Processing, 2021, 810, 140985.	2.6	27
276	Compaction behavior of water-atomized CoCrFeMnNi high-entropy alloy powders. Materials Chemistry and Physics, 2018, 210, 95-102.	2.0	27
277	Architectured heterogeneous alloys with selective laser melting. Scripta Materialia, 2022, 208, 114332.	2.6	27
278	Finite element analysis of compressive deformation of bulk metallic glasses. Acta Materialia, 2004, 52, 3813-3823.	3.8	26
279	A semi-phenomenological constitutive model for hcp materials as exemplified by alpha titanium. Scripta Materialia, 2012, 67, 121-124.	2.6	26
280	Mechanical properties and microstructure evolution in ultrafine-grained AZ31 alloy processed by severe plastic deformation. Journal of Materials Science, 2013, 48, 4705-4712.	1.7	26
281	Analysis of plastic deformation behavior during back pressure equal channel angular pressing by the finite element method. Computational Materials Science, 2013, 77, 202-207.	1.4	26
282	Correlation Between Microstructures and Tensile Properties of Strain-Based API X60 Pipeline Steels. Metallurgical and Materials Transactions A: Physical Metallurgy and Materials Science, 2016, 47, 2726-2738.	1.1	26
283	Nanoporous High-Entropy Alloy by Liquid Metal Dealloying. Metals, 2020, 10, 1396.	1.0	26
284	2.3 GPa cryogenic strength through thermal-induced and deformation-induced body-centered cubic martensite in a novel ferrous medium entropy alloy. Scripta Materialia, 2021, 204, 114157.	2.6	26
285	Gradient-structured high-entropy alloy with improved combination of strength and hydrogen embrittlement resistance. Corrosion Science, 2022, 200, 110253.	3.0	26
286	Thermo-mechanical processing and properties of Cu–9Fe–1.2Co microcomposite wires. Scripta Materialia, 2001, 45, 1295-1300.	2.6	25
287	Finite Element Analysis of the Onset of Necking and the Post-Necking Behaviour during Uniaxial Tensile Testing. Materials Transactions, 2005, 46, 2159-2163.	0.4	25
288	Effect of C content on the microstructure and tensile properties of lightweight ferritic Fe-8Al-5Mn-0.1Nb alloy. Metals and Materials International, 2015, 21, 79-84.	1.8	25

#	Article	IF	CITATIONS
289	Development of an Advanced Ultrahigh Strength TRIP Steel and Evaluation of Its Unique Strain Hardening Behavior. Metals and Materials International, 2020, 26, 168-178.	1.8	25
290	Cold spray deposition characteristic and bonding of CrMnCoFeNi high entropy alloy. Surface and Coatings Technology, 2021, 425, 127748.	2.2	25
291	Microstructure and Mechanical Properties of Copper Processed by Twist Extrusion with a Reduced Twist-Line Slope. Metallurgical and Materials Transactions A: Physical Metallurgy and Materials Science, 2014, 45, 2232-2241.	1.1	24
292	Three-dimensional real structure-based finite element analysis of mechanical behavior for porous titanium manufactured by a space holder method. Computational Materials Science, 2015, 100, 2-7.	1.4	24
293	Metal Deposition on a Selfâ€Generated Microfibril Network to Fabricate Stretchable Tactile Sensors Providing Analog Position Information. Advanced Materials, 2018, 30, e1801408.	11.1	24
294	Ultra-high strength and excellent ductility in multi-layer steel sheet of austenitic hadfield and martensitic hot-press-forming steels. Materials Science & Engineering A: Structural Materials: Properties, Microstructure and Processing, 2019, 759, 320-328.	2.6	24
295	Superior-tensile property of CoCrFeMnNi alloys achieved using friction-stir welding for cryogenic applications. Materials Science & Engineering A: Structural Materials: Properties, Microstructure and Processing, 2020, 788, 139547.	2.6	24
296	Super-resolving material microstructure image via deep learning for microstructure characterization and mechanical behavior analysis. Npj Computational Materials, 2021, 7, .	3.5	24
297	Superior antifouling properties of a CoCrFeMnNi high-entropy alloy. Materials Letters, 2021, 300, 130130.	1.3	24
298	Finite element analysis of rotary-die equal channel angular pressing. Materials Science & Engineering A: Structural Materials: Properties, Microstructure and Processing, 2008, 490, 289-292.	2.6	23
299	In situ synthesis of nanocrystalline Al6063 matrix nanocomposite powder via reactive mechanical alloying. Materials Science & Engineering A: Structural Materials: Properties, Microstructure and Processing, 2010, 527, 4897-4905.	2.6	23
300	Effects of Inclusions on Delayed Fracture Properties of Three TWinning Induced Plasticity (TWIP) Steels. Metallurgical and Materials Transactions A: Physical Metallurgy and Materials Science, 2013, 44, 776-786.	1.1	23
301	Quasi-static and dynamic compressive deformation behaviors in Zr-based amorphous alloys containing ductile dendrites. Materials Science & Engineering A: Structural Materials: Properties, Microstructure and Processing, 2013, 579, 77-85.	2.6	23
302	Finite element analysis of the effect of friction in high pressure torsion. Metals and Materials International, 2014, 20, 445-450.	1.8	23
303	Tensile properties of cold-rolled TWIP-cored three-layer steel sheets. Materials Science & Engineering A: Structural Materials: Properties, Microstructure and Processing, 2017, 686, 160-167.	2.6	23
304	Threshold Voltage Drift in Te-Based Ovonic Threshold Switch Devices Under Various Operation Conditions. IEEE Electron Device Letters, 2020, 41, 191-194.	2.2	23
305	Plastic Deformation and Computer Simulations of Equal Channel Angular Pressing. Journal of Korean Institute of Metals and Materials, 2014, 52, 87-99.	0.4	23
306	Strengthening the mechanical properties and wear resistance of CoCrFeMnNi high entropy alloy fabricated by powder metallurgy. Advanced Powder Technology, 2022, 33, 103519.	2.0	23

#	Article	IF	CITATIONS
307	Heterostructured alloys with enhanced strength-ductility synergy through laser-cladding. Scripta Materialia, 2022, 215, 114732.	2.6	23
308	Hot deformation of ultrafine-grained Al6063/Al2O3 nanocomposites. Journal of Materials Science, 2011, 46, 4994-5001.	1.7	22
309	X-ray diffraction study on the microstructure of a Mg–Zn–Y alloy consolidated by high-pressure torsion. Journal of Alloys and Compounds, 2012, 539, 32-35.	2.8	22
310	Effects of microstructure and pipe forming strain on yield strength before and after spiral pipe forming of API X70 and X80 linepipe steel sheets. Materials Science & Engineering A: Structural Materials: Properties, Microstructure and Processing, 2013, 573, 18-26.	2.6	22
311	Mechanisms of toughness improvement in Charpy impact and fracture toughness tests of non-heat-treating cold-drawn steel bar. Materials Science & Engineering A: Structural Materials: Properties, Microstructure and Processing, 2013, 571, 38-48.	2.6	22
312	Three-Dimensional Characterization of SiC Particle-Reinforced Al Composites Using Serial Sectioning Tomography and Thermo-mechanical Finite Element Simulation. Metallurgical and Materials Transactions A: Physical Metallurgy and Materials Science, 2014, 45, 5679-5690.	1.1	22
313	Simple shear model of twist extrusion and its deviations. Metals and Materials International, 2015, 21, 569-579.	1.8	22
314	Effect of the fabrication method on the wear properties of copper silicon carbide composites. Tribology International, 2018, 128, 140-154.	3.0	22
315	The high temperature mechanical properties and the correlated microstructure/ texture evolutions of a TWIP high entropy alloy. Materials Science & Engineering A: Structural Materials: Properties, Microstructure and Processing, 2021, 802, 140600.	2.6	22
316	Multi-layered gradient structure manufactured by single-roll angular-rolling and ultrasonic nanocrystalline surface modification. Scripta Materialia, 2020, 186, 52-56.	2.6	22
317	Densification mechanisms during hot isostatic pressing of stainless steel powder compacts. Journal of Materials Processing Technology, 2002, 123, 319-322.	3.1	21
318	Mechanical properties of equal channel angular pressed powder extrudates of a rapidly solidified hypereutectic Al-20wt% Si alloy. Materials Science & Engineering A: Structural Materials: Properties, Microstructure and Processing, 2007, 449-451, 966-970.	2.6	21
319	Flexural Test for Steel-Concrete Composite Members Using Prefabricated Steel Angles. Journal of Structural Engineering, 2014, 140, .	1.7	21
320	Torsional and compressive behaviours of a hybrid material: Spiral fibre reinforced metal matrix composite. Materials and Design, 2015, 85, 404-411.	3.3	21
321	Compressive behavior of NiTi-based composites reinforced with alumina nanoparticles. Journal of Alloys and Compounds, 2016, 688, 803-807.	2.8	21
322	Effects of homogenization temperature on cracking during cold-rolling of Al0.5CoCrFeMnNi high-entropy alloy. Materials Chemistry and Physics, 2018, 210, 187-191.	2.0	21
323	Fabrication of Mg/Al12Mg17 in-situ surface nanocomposite via friction stir processing. Materials Science & Engineering A: Structural Materials: Properties, Microstructure and Processing, 2018, 712, 655-662.	2.6	21
324	Effect of Initial Grain Size on Deformation Mechanism during Highâ€Pressure Torsion in V 10 Cr 15 Mn 5 Fe 35 Co 10 Ni 25 Highâ€Entropy Alloy. Advanced Engineering Materials, 2020, 22, 1900587.	1.6	21

#	Article	IF	CITATIONS
325	Novel precipitation and enhanced tensile properties in selective laser melted Cu-Sn alloy. Materialia, 2020, 13, 100861.	1.3	21
326	Effects of grain size on body-centered-cubic martensitic transformation in metastable Fe46Co30Cr10Mn5Si7V2 high-entropy alloy. Scripta Materialia, 2021, 194, 113620.	2.6	21
327	Beyond strength-ductility trade-off: 3D interconnected heterostructured composites by liquid metal dealloying. Composites Part B: Engineering, 2021, 225, 109266.	5.9	21
328	Lattice vibrational properties of ZnMgO grown by pulsed laser deposition. Applied Physics Letters, 2007, 90, 192110.	1.5	20
329	Processing and Mechanical Properties of Fine Grained Magnesium by Equal Channel Angular Pressing. Materials Transactions, 2008, 49, 1006-1010.	0.4	20
330	The Effects of a Stabilizer Thickness of the YBCO Coated Conductor (CC) on the Quench/Recovery Characteristics. IEEE Transactions on Applied Superconductivity, 2010, 20, 1246-1249.	1.1	20
331	A plastic-yield compaction model for nanostructured Al6063 alloy and Al6063/Al2O3 nanocomposite powder. Powder Technology, 2011, 211, 215-220.	2.1	20
332	Mechanical properties and thermal stability of bulk Cu cold consolidated from atomized powders by high-pressure torsion. Journal of Materials Science, 2012, 47, 7770-7776.	1.7	20
333	An Investigation on the Fatigue Fracture of P/M Al-SiC Nanocomposites. Metallurgical and Materials Transactions A: Physical Metallurgy and Materials Science, 2013, 44, 2662-2671.	1.1	20
334	Contributions of different strengthening mechanisms to the shear strength of an extruded Mg–4Zn–0.5Ca alloy. Philosophical Magazine, 2015, 95, 3452-3466.	0.7	20
335	Microstructural and kinetic investigation on the suppression of grain growth in nanocrystalline copper by the dispersion of silicon carbide nanoparticles. Materials and Design, 2017, 119, 311-318.	3.3	20
336	Intragranular Dispersion of Carbon Nanotubes Comprehensively Improves Aluminum Alloys. Advanced Science, 2018, 5, 1800115.	5.6	20
337	The Effect of Processing Route on Properties of HfNbTaTiZr High Entropy Alloy. Materials, 2019, 12, 4022.	1.3	20
338	Mechanical property enhancement in gradient structured aluminum alloy by ultrasonic nanocrystalline surface modification. Materials Science & Engineering A: Structural Materials: Properties, Microstructure and Processing, 2021, 812, 141101.	2.6	20
339	Microstructural characterization and enhanced hardness of nanostructured Ni3Ti– NiTi (B2) intermetallic alloy produced by mechanical alloying and fast microwave-assisted sintering process. Intermetallics, 2021, 131, 107119.	1.8	20
340	Synergetic strengthening from grain refinement and nano-scale precipitates in non-equiatomic CoCrFeNiMo medium-entropy alloy. Intermetallics, 2021, 135, 107212.	1.8	20
341	Effects of Laser Power on the Microstructure Evolution and Mechanical Properties of Ti–6Al–4V Alloy Manufactured by Direct Energy Deposition. Metals and Materials International, 2022, 28, 197-204.	1.8	20
342	Defects in High Entropy Alloy HfNbTaTiZr Prepared by High Pressure Torsion. Acta Physica Polonica A, 2018, 134, 891-894.	0.2	20

#	Article	IF	CITATIONS
343	Effects of deformation-induced martensitic transformation on cryogenic fracture toughness for metastable Si8V2Fe45Cr10Mn5Co30 high-entropy alloy. Acta Materialia, 2022, 225, 117568.	3.8	20
344	Strengthening mechanisms of Zr-based devitrified amorphous alloy nanocomposites. Scripta Materialia, 2003, 48, 43-49.	2.6	19
345	On the effect of acute angles on deformation homogeneity in equal channel angular pressing. Materials Science & Engineering A: Structural Materials: Properties, Microstructure and Processing, 2006, 430, 346-349.	2.6	19
346	Finite-element analysis for high-temperature deformation of bulk metallic glasses in a supercooled liquid region based on the free volume constitutive model. Acta Materialia, 2010, 58, 4267-4280.	3.8	19
347	Deformation behavior in the tubular channel angular pressing (TCAP) as a noble SPD method for cylindrical tubes. Applied Physics A: Materials Science and Processing, 2012, 107, 819-827.	1.1	19
348	Finite element analysis for the geometry effect on strain inhomogeneity during high-pressure torsion. Journal of Materials Science, 2014, 49, 6620-6628.	1.7	19
349	Microstructure and high-temperature mechanical properties of the Mg–4Zn–0.5Ca alloy in the as-cast and aged conditions. Materials Science & Engineering A: Structural Materials: Properties, Microstructure and Processing, 2016, 649, 441-448.	2.6	19
350	Effect of initial grain size on the microstructure and mechanical properties of high-pressure torsion processed twinning-induced plasticity steels. Materials Science & Engineering A: Structural Materials: Properties, Microstructure and Processing, 2017, 682, 164-167.	2.6	19
351	Prediction of hole expansion ratio for various steel sheets based on uniaxial tensile properties. Metals and Materials International, 2018, 24, 187-194.	1.8	19
352	Outstanding mechanical properties of ultrafine-grained Al7075 alloys by high-pressure torsion. Materials Science & Engineering A: Structural Materials: Properties, Microstructure and Processing, 2021, 810, 141020.	2.6	19
353	Fabrication of multi-gradient heterostructured CoCrFeMnNi high-entropy alloy using laser metal deposition. Materials Science & Engineering A: Structural Materials: Properties, Microstructure and Processing, 2022, 836, 142718.	2.6	19
354	Finite element analysis of torsional deformation. Materials Science & Engineering A: Structural Materials: Properties, Microstructure and Processing, 2001, 299, 305-308.	2.6	18
355	Densification modelling for nanocrystalline metallic powders. Journal of Materials Processing Technology, 2003, 140, 401-406.	3.1	18
356	Strength and strain hardening of nanocrystalline materials. Materials Science & Engineering A: Structural Materials: Properties, Microstructure and Processing, 2008, 483-484, 127-130.	2.6	18
357	Analysis of stress states in compression stage of high pressure torsion using slab analysis method and finite element method. Metals and Materials International, 2013, 19, 1021-1027.	1.8	18
358	Correlative Highâ€Resolution Mapping of Strain and Charge Density in a Strained Piezoelectric Multilayer. Advanced Materials Interfaces, 2015, 2, 1400281.	1.9	18
359	Effects of Annealing Treatment Prior to Cold Rolling on Delayed Fracture Properties in Ferrite-Austenite Duplex Lightweight Steels. Metallurgical and Materials Transactions A: Physical Metallurgy and Materials Science, 2016, 47, 706-717.	1.1	18
360	Fabrication of Fullerene-Reinforced Aluminum Matrix Nanocomposites. Acta Metallurgica Sinica (English Letters), 2017, 30, 973-982.	1.5	18

#	Article	IF	CITATIONS
361	Deep Drawing Behavior of CoCrFeMnNi High-Entropy Alloys. Metallurgical and Materials Transactions A: Physical Metallurgy and Materials Science, 2017, 48, 4111-4120.	1.1	18
362	Shape memory characteristics of a nanocrystalline TiNi alloy processed by HPT followed by post-deformation annealing. Materials Science & Engineering A: Structural Materials: Properties, Microstructure and Processing, 2018, 734, 445-452.	2.6	18
363	An approach for screening single phase high-entropy alloys using an in-house thermodynamic database. Intermetallics, 2018, 101, 56-63.	1.8	18
364	Precipitation behaviour and mechanical properties of a new wrought high entropy superalloy. Materials Science & Engineering A: Structural Materials: Properties, Microstructure and Processing, 2019, 749, 271-280.	2.6	18
365	Design of a Janusâ€Faced Electrode for Highly Stretchable Zinc–Silver Rechargeable Batteries. Advanced Functional Materials, 2020, 30, 2004137.	7.8	18
366	On the phase transformation and dynamic stress–strain partitioning of ferrous medium-entropy alloy using experimentation and finite element method. Materialia, 2020, 9, 100619.	1.3	18
367	Synergetic strengthening of additively manufactured (CoCrFeMnNi)99C1 high-entropy alloy by heterogeneous anisotropic microstructure. Additive Manufacturing, 2020, 35, 101333.	1.7	18
368	Developing harmonic structure in CoCrFeMnNi high entropy alloy to enhance mechanical properties via powder metallurgy approach. Journal of Materials Research and Technology, 2022, 17, 1686-1695.	2.6	18
369	Influence of arsenic during indium deposition on the formation of the wetting layers of InAs quantum dots grown by migration enhanced epitaxy. Journal of Applied Physics, 2004, 96, 4122-4125.	1.1	17
370	Analysis of T-Shaped Equal Channel Angular Pressing using the Finite Element Method. Metals and Materials International, 2008, 14, 565-568.	1.8	17
371	Plastic deformation and microstructural evolution during the shock consolidation of ultrafine copper powders. Materials Science & Engineering A: Structural Materials: Properties, Microstructure and Processing, 2015, 625, 230-244.	2.6	17
372	High-temperature thermo-mechanical behavior of functionally graded materials produced by plasma sprayed coating: Experimental and modeling results. Metals and Materials International, 2016, 22, 817-824.	1.8	17
373	Large deformation behavior of twin-induced plasticity steels under high-pressure torsion. Metals and Materials International, 2016, 22, 1003-1008.	1.8	17
374	Modeling and Characterization of Texture Evolution in Twist Extrusion. Metallurgical and Materials Transactions A: Physical Metallurgy and Materials Science, 2016, 47, 1248-1260.	1.1	17
375	On the rule-of-mixtures of the hardening parameters in TWIP-cored three-layer steel sheet. Metals and Materials International, 2017, 23, 459-464.	1.8	17
376	Numerical analysis on the formation of P-orientation near coarse precipitates in FCC crystals during recrystallization. Acta Materialia, 2017, 131, 363-372.	3.8	17
377	Equivalent strain at large shear deformation: Theoretical, numerical and finite element analysis. Journal of Applied Research and Technology, 2017, 15, 442-448.	0.6	17
378	Unusual strain-induced martensite and absence of conventional grain refinement in twinning induced plasticity high-entropy alloy processed by high-pressure torsion. Materials Science & Engineering A: Structural Materials: Properties, Microstructure and Processing, 2021, 803, 140570.	2.6	17

#	Article	IF	CITATIONS
379	Anomalous compliance of interpenetrating-phase composite of Ti and Mg synthesized by liquid metal dealloying. Scripta Materialia, 2021, 194, 113660.	2.6	17
380	The subsurface deformed region and superficial protective tribo-oxide layer during wear in a non-equiatomic CoCrFeNiV high entropy alloy. Materials and Design, 2022, 218, 110685.	3.3	17
381	Nanostructure Formation in Copper Subjected to High Pressure Torsion. Defect and Diffusion Forum, 2002, 208-209, 229-232.	0.4	16
382	Process Modelling of Equal Channel Angular Pressing for Ultrafine Grained Materials. Materials Transactions, 2004, 45, 2172-2176.	0.4	16
383	Equal Channel Angular Pressing of Carbon Nanotube Reinforced Metal Matrix Nanocomposites. Key Engineering Materials, 2006, 326-328, 325-328.	0.4	16
384	The effects of alloying and pressing routes in equal channel angular pressing of Cu-Fe-Cr and Cu-Fe-Cr Ag composites. Metals and Materials International, 2009, 15, 733-739.	1.8	16
385	Simulation and experimental analyses of dynamic strain aging of a supersaturated age hardenable aluminum alloy. Materials Science & Engineering A: Structural Materials: Properties, Microstructure and Processing, 2013, 585, 165-173.	2.6	16
386	Estimating interface bonding strength in clad metals using digital image correlation. Scripta Materialia, 2013, 68, 893-896.	2.6	16
387	Effects of Effective Dendrite Size on Tensile Deformation Behavior in Ti-Based Dendrite-Containing Amorphous Matrix Composites Modified from Ti-6Al-4V Alloy. Metallurgical and Materials Transactions A: Physical Metallurgy and Materials Science, 2015, 46, 235-250.	1.1	16
388	Microstructure and Mechanical Properties of Ultra-fine-Grained Al-Mg-Si Tubes Produced by Parallel Tubular Channel Angular Pressing Process. Metallurgical and Materials Transactions A: Physical Metallurgy and Materials Science, 2015, 46, 1805-1813.	1.1	16
389	Off-axis twist extrusion for uniform processing of round bars. Metals and Materials International, 2015, 21, 734-740.	1.8	16
390	Residual Stress Effect on the Delayed Fracture of Twinning-Induced Plasticity Steels. Metallurgical and Materials Transactions A: Physical Metallurgy and Materials Science, 2017, 48, 2692-2696.	1.1	16
391	Microstructure development of ultra fine grained Mg-22 wt%Gd alloy prepared by high pressure torsion. Materials Science & Engineering A: Structural Materials: Properties, Microstructure and Processing, 2017, 704, 181-191.	2.6	16
392	Superplasticity of V10Cr15Mn5Fe35Co10Ni25 high-entropy alloy processed using high-pressure torsion. Materials Science & Engineering A: Structural Materials: Properties, Microstructure and Processing, 2019, 764, 138198.	2.6	16
393	Effects of strain rate on room- and cryogenic-temperature compressive properties in metastable V10Cr10Fe45Co35 high-entropy alloy. Scientific Reports, 2019, 9, 6163.	1.6	16
394	Novel Co-Cu-Based Immiscible Medium-Entropy Alloys with Promising Mechanical Properties. Metals, 2021, 11, 238.	1.0	16
395	Gradient-structured ferrous medium-entropy alloys with enhanced strength-ductility synergy by ultrasonic nanocrystalline surface modification. Materials Science & Engineering A: Structural Materials: Properties, Microstructure and Processing, 2021, 826, 141966.	2.6	16
396	Metastability engineering of partially recrystallized C-doped non-equiatomic CoCrFeNiMo medium-entropy alloy. Applied Physics Letters, 2021, 119, .	1.5	16

#	Article	IF	CITATIONS
397	Microstructure and defect effects on strength and hydrogen embrittlement of high-entropy alloy CrMnFeCoNi processed by high-pressure torsion. Materials Science & Engineering A: Structural Materials: Properties, Microstructure and Processing, 2022, 844, 143179.	2.6	16
398	Analysis of Coefficient of Friction in Compression of Porous Metal Rings. Powder Metallurgy, 1994, 37, 259-264.	0.9	15
399	Materials and Process Development for ZnMgO/ZnO Light-Emitting Diodes. IEEE Journal of Selected Topics in Quantum Electronics, 2008, 14, 1048-1052.	1.9	15
400	Annealing effects on electrical properties of MgZnO films grown by pulsed laser deposition. Journal of Applied Physics, 2008, 103, 083704.	1.1	15
401	Coupled Analysis of Heat Transfer and Deformation in Equal Channel Angular Pressing of Al and Steel. Materials Transactions, 2009, 50, 40-43.	0.4	15
402	Hollow cone high-pressure torsion: Microstructure and tensile strength by unique severe plastic deformation. Scripta Materialia, 2014, 71, 41-44.	2.6	15
403	Effect of high-pressure torsion on the microstructure and wear behavior of NiTi alloy. Metals and Materials International, 2015, 21, 891-896.	1.8	15
404	Thickness inhomogeneity in hardness and microstructure of copper after the compressive stage in high-pressure torsion. Metals and Materials International, 2015, 21, 7-13.	1.8	15
405	Using dilatometry to study martensitic stabilization and recrystallization kinetics in a severely deformed NiTi alloy. Journal of Materials Science, 2015, 50, 4003-4011.	1.7	15
406	Threshold creep behaviour of an aged Mg–Zn–Ca alloy. Materials Science & Engineering A: Structural Materials: Properties, Microstructure and Processing, 2017, 696, 536-543.	2.6	15
407	Dynamic tensile behavior of twinning-induced plasticity/low-carbon (TWIP/LC) steel clad sheets bonded by hot rolling. Materials Science & Engineering A: Structural Materials: Properties, Microstructure and Processing, 2017, 700, 387-396.	2.6	15
408	Severe Plastic Deformation Methods for Sheets. , 2018, , 113-129.		15
409	Excellent combination of cryogenic-temperature strength and ductility of high-entropy-alloy-cored multi-layered sheet. Journal of Alloys and Compounds, 2019, 797, 465-470.	2.8	15
410	The enhancement of transformation induced plasticity effect through preferentially oriented substructure development in a high entropy alloy. Intermetallics, 2019, 109, 145-156.	1.8	15
411	Effects of processing parameters and heat treatment on the microstructure and magnetic properties of the in-situ synthesized Fe-Ni permalloy produced using direct energy deposition. Journal of Alloys and Compounds, 2022, 907, 164415.	2.8	15
412	A facile strengthening method by co-doping boron and nitrogen in CoCrFeMnNi high-entropy alloy. Materials Science & Engineering A: Structural Materials: Properties, Microstructure and Processing, 2022, 846, 143307.	2.6	15
413	Power-law creep model for densification of powder compacts. Materials Science & Engineering A: Structural Materials: Properties, Microstructure and Processing, 1999, 271, 424-429.	2.6	14
414	Formation of 2–5 nm size pre-precipitates of cF96 phase in a Hf–Co–Al glassy alloy. Journal of Alloys and Compounds, 2003, 359, 198-201.	2.8	14

#	Article	IF	CITATIONS
415	Finite element analysis of the bending behavior of a workpiece in equal channel angular pressing. Metals and Materials International, 2009, 15, 215-219.	1.8	14
416	Upper bound analysis of deformation and dynamic ageing behavior in elevated temperature equal channel angular pressing of Al-Mg-Si alloys. Metals and Materials International, 2010, 16, 363-369.	1.8	14
417	Forming Nanocrystalline Structures in Metal Particle Impact. Metallurgical and Materials Transactions A: Physical Metallurgy and Materials Science, 2011, 42, 3006-3012.	1.1	14
418	Nanoindentation analysis for local properties of ultrafine grained copper processed by high pressure torsion. Journal of Materials Science, 2012, 47, 7828-7834.	1.7	14
419	Hardness and microstructure of interstitial free steels in the early stage of high-pressure torsion. Journal of Materials Science, 2013, 48, 4698-4704.	1.7	14
420	Residual Stress Analysis in Deep Drawn Twinning Induced Plasticity (TWIP) Steels Using Neutron Diffraction Method. Metallurgical and Materials Transactions A: Physical Metallurgy and Materials Science, 2014, 45, 1953-1961.	1.1	14
421	Experimental and finite element analyses of plastic deformation behavior in vortex extrusion. Materials Science & Engineering A: Structural Materials: Properties, Microstructure and Processing, 2016, 674, 472-479.	2.6	14
422	Neutron diffraction and finite element analysis of the residual stress distribution of copper processed by equal-channel angular pressing. Materials Science & Engineering A: Structural Materials: Properties, Microstructure and Processing, 2017, 682, 691-697.	2.6	14
423	Molybdenum Disulfide Surface Modification of Ultrafine-Grained Titanium for Enhanced Cellular Growth and Antibacterial Effect. Scientific Reports, 2018, 8, 9907.	1.6	14
424	Effect of grain size on stretch-flangeability of twinning-induced plasticity steels. Materials Science & Engineering A: Structural Materials: Properties, Microstructure and Processing, 2018, 735, 295-301.	2.6	14
425	Synergetic strengthening of layered steel sheet investigated using an in situ neutron diffraction tensile test. Scientific Reports, 2019, 9, 6829.	1.6	14
426	Body-centered-cubic martensite and the role on room-temperature tensile properties in Si-added SiVCrMnFeCo high-entropy alloys. Journal of Materials Science and Technology, 2021, 76, 222-230.	5.6	14
427	Correlation between microstructural heterogeneity and mechanical properties of WC-Co composite additively manufactured by selective laser melting. Materials Letters, 2021, 293, 129683.	1.3	14
428	Superior strain-hardening by deformation-induced nano-HCP martensite in Fe–Mn–Si–C high-manganese steel. Materials Science & Engineering A: Structural Materials: Properties, Microstructure and Processing, 2021, 824, 141864.	2.6	14
429	Corrosion-resistant Cu-Fe-based immiscible medium-entropy alloy with tri-layer passivation. Corrosion Science, 2021, 193, 109888.	3.0	14
430	Isothermal nanocrystallisation behaviour of melt spun Al86Ni9Mm5(Mmmischmetal)amorphous alloy. Materials Science and Technology, 2003, 19, 966-972.	0.8	13
431	Molecular dynamics study on local structure of amorphous and liquid Al2O3. Metals and Materials International, 2006, 12, 167-172.	1.8	13
432	Equal Channel Angular Pressing of Metallic Powders for Nanostructured Materials. Materials Science Forum, 2006, 503-504, 221-226.	0.3	13

#	Article	IF	CITATIONS
433	Mechanical properties of commercially pure aluminium subjected to repetitive bending and straightening process. Transactions of the Indian Institute of Metals, 2008, 61, 165-167.	0.7	13
434	Amorphous phase formation in Al80Fe10M10 (MÂ=ÂNi, Ti, and V) ternary systems by mechanical alloying. Journal of Materials Science, 2011, 46, 7633-7638.	1.7	13
435	High-temperature deformation and structural restoration of a nanostructured Al alloy. Scripta Materialia, 2012, 66, 911-914.	2.6	13
436	Microstructure Evolution and Mechanical Properties of Al-1080 Processed by a Combination of Equal Channel Angular Pressing and High Pressure Torsion. Metallurgical and Materials Transactions A: Physical Metallurgy and Materials Science, 2013, 44, 2581-2590.	1.1	13
437	Comparative Analysis of Two Twist-Based SPD Processes: Elliptical Cross-Section Spiral Equal-Channel Extrusion vs. Twist Extrusion. Materials Transactions, 2013, 54, 1587-1591.	0.4	13
438	Characterizations of dissimilar friction welding of ST37 and CK60 steels. International Journal of Advanced Manufacturing Technology, 2016, 85, 2773-2781.	1.5	13
439	Investigation of direct extrusion channel effects on twist extrusion using experimental and finite element analysis. Measurement: Journal of the International Measurement Confederation, 2018, 127, 115-123.	2.5	13
440	Micromechanical analysis of orientation dependency on deformation behavior in DP steels by dislocation density-based crystal plasticity simulation. Mechanics of Materials, 2019, 134, 132-142.	1.7	13
441	Tailoring Extra-Strength of a TWIP Steel by Combination of Multi-Pass Equal-Channel Angular Pressing and Warm Rolling. Metals, 2021, 11, 518.	1.0	13
442	Twinning engineering of high-entropy alloys: An exercise in process optimization and modeling. Materials Science & Engineering A: Structural Materials: Properties, Microstructure and Processing, 2021, 822, 141681.	2.6	13
443	Microstructural evolution and mechanical properties of nanocrystalline Fe–Mn–Al–C steel processed by high-pressure torsion. Materials Science & Engineering A: Structural Materials: Properties, Microstructure and Processing, 2021, 827, 142073.	2.6	13
444	Superior phase transformation-assisted mechanical properties of a metastable medium-entropy ferrous alloy with heterogeneous microstructure. Materials Letters, 2021, 302, 130391.	1.3	13
445	Delayed deformation-induced martensite transformation and enhanced cryogenic tensile properties in laser additive manufactured 316L austenitic stainless steel. Additive Manufacturing, 2021, 47, 102314.	1.7	13
446	TiC-reinforced CoCrFeMnNi composite processed by cold-consolidation and subsequent annealing. Materials Letters, 2021, 303, 130503.	1.3	13
447	On the development of a novel multi-phase highÂentropy alloy with transformation-induced plasticity effect. Journal of Alloys and Compounds, 2022, 905, 164014.	2.8	13
448	Free volume formation and the high strength of pure Mg after room temperature core-sheath ECAP passes. Journal of Materials Research and Technology, 2022, 18, 147-158.	2.6	13
449	Plastic deformation of porous metal with an initial inhomogeneous density distribution. Journal of Materials Processing Technology, 1998, 74, 213-217.	3.1	12
450	Modeling of aluminum via filling by forcefill. Journal of Applied Physics, 2003, 93, 5812-5815.	1.1	12

#	Article	IF	CITATIONS
451	Tensile properties of electrodeposited nanocrystalline nickel. Materials Science & Engineering A: Structural Materials: Properties, Microstructure and Processing, 2007, 449-451, 836-840.	2.6	12
452	Constitutive Modeling of Hot Deformation Behavior of the AA6063 Alloy with Different Precipitates. Metallurgical and Materials Transactions A: Physical Metallurgy and Materials Science, 2013, 44, 5853-5860.	1.1	12
453	An upper bound solution for twist extrusion process. Metals and Materials International, 2014, 20, 825-834.	1.8	12
454	Effect of the interfacial condition on the microtexture near the interface of Al/Cu composites during multi-pass caliber rolling. Materials and Design, 2015, 82, 28-36.	3.3	12
455	Toward architecturing of metal composites by twist extrusion. Materials Research Letters, 2015, 3, 161-168.	4.1	12
456	Consolidation of Cu-based amorphous alloy powders by high-pressure torsion. Journal of Materials Science, 2015, 50, 3164-3174.	1.7	12
457	Mechanical and biological behavior of ultrafine-grained Ti alloy aneurysm clip processed using high-pressure torsion. Journal of the Mechanical Behavior of Biomedical Materials, 2017, 68, 203-209.	1.5	12
458	Novel twin-roll-cast Ti/Al clad sheets with excellent tensile properties. Scientific Reports, 2017, 7, 8110.	1.6	12
459	Interpretation of dynamic tensile behavior by austenite stability in ferrite-austenite duplex lightweight steels. Scientific Reports, 2017, 7, 15726.	1.6	12
460	Effect of coarse precipitates on surface roughening of an FCC polycrystalline material using crystal plasticity. Computational Materials Science, 2017, 126, 121-131.	1.4	12
461	Modelling the evolution of recrystallization texture for a non-grain oriented electrical steel. Computational Materials Science, 2018, 149, 57-64.	1.4	12
462	Microstructural tailoring in reverse gradient-structured copper sheet using single-roll angular-rolling and subsequent annealing. Materials Science & Engineering A: Structural Materials: Properties, Microstructure and Processing, 2019, 764, 138258.	2.6	12
463	Microstructural behavior and mechanical properties of nanocrystalline Ti-22Al-25Nb alloy processed by high-pressure torsion. Materials Characterization, 2019, 151, 129-136.	1.9	12
464	Effects of Si on the Microstructure and Work Hardening Behavior of Fe‒17Mn‒1.1C‒xSi High Manganese Steels. Metals and Materials International, 2021, 27, 3891-3904.	1.8	12
465	Forecast of Adiabatic Shear Band Formation in Two Commercial Ultra-high-Strength Armor Steels by Split Hopkinson Pressure Bar. Metallurgical and Materials Transactions A: Physical Metallurgy and Materials Science, 2020, 51, 3384-3391.	1.1	12
466	Hetero-deformation-induced strengthening of multi-phase Cu–Fe–Mn medium entropy alloys by dynamic heterostructuring. Materials Science & Engineering A: Structural Materials: Properties, Microstructure and Processing, 2021, 799, 140275.	2.6	12
467	Obtaining a Wide-Strain-Range True Stress–Strain Curve Using the Measurement-In-Neck-Section Method. Experimental Mechanics, 2021, 61, 1343-1348.	1.1	12
468	Effect of heat treatment on the mechanical properties and microstructure of HSLA steels processed by various technologies. Materials Today Communications, 2021, 28, 102598.	0.9	12

#	Article	IF	CITATIONS
469	Airâ€Permeable Waterproofing Electrocardiogram Patch to Monitor Fullâ€Day Activities for Multiple Days. Advanced Healthcare Materials, 2022, 11, e2102703.	3.9	12
470	Superlative room temperature and cryogenic tensile properties of nanostructured CoCrFeNi medium-entropy alloy fabricated by powder high-pressure torsion. Scripta Materialia, 2022, 213, 114631.	2.6	12
471	Fe55Co17.5Ni10Cr12.5Mo5 High-Entropy Alloy with Outstanding Cryogenic Mechanical Properties Driven by Deformation-Induced Phase Transformation Behavior. Metals and Materials International, 2023, 29, 95-107.	1.8	12
472	Densification of sintered porous metal under hydrostatic pressure. Scripta Metallurgica Et Materialia, 1993, 29, 1211-1216.	1.0	11
473	Strength and ductility of heavily drawn bundled Cu-Nb filamentary microcomposite wires with various Nb contents. Metallurgical and Materials Transactions A: Physical Metallurgy and Materials Science, 2000, 31, 2457-2462.	1.1	11
474	Mechanical Modeling of Al-Mg Alloy Open-Cell Foams. Materials Transactions, 2005, 46, 622-625.	0.4	11
475	Comparison in Deformation and Fracture Behavior of Magnesium during Equal Channel Angular Pressing by Experimental and Numerical Methods. Materials Transactions, 2008, 49, 963-966.	0.4	11
476	Analysis of thermal behavior during equal channel multi-angular pressing by the 3-dimensional finite volume method. Materials Science & Engineering A: Structural Materials: Properties, Microstructure and Processing, 2009, 503, 130-136.	2.6	11
477	Dynamic Compressive Properties of Zr-based Amorphous Matrix Composites Reinforced with Tungsten Continuous Fibers or Porous Foams. Metallurgical and Materials Transactions A: Physical Metallurgy and Materials Science, 2012, 43, 1911-1920.	1.1	11
478	Structural, luminescent, and NO2 sensing properties of SnO2-core/V2O5-shell nanorods. Journal of Electroceramics, 2013, 30, 6-12.	0.8	11
479	Bandgap Tuning with Thermal Residual Stresses Induced in a Quantum Dot. Small, 2014, 10, 3678-3684.	5.2	11
480	Finite Element and Experimental Analysis of Closure and Contact Bonding of Pores During Hot Rolling of Steel. Metallurgical and Materials Transactions A: Physical Metallurgy and Materials Science, 2014, 45, 4002-4011.	1.1	11
481	Enhanced wear resistivity of a Zr-based bulk metallic glass processed by high-pressure torsion under reciprocating dry conditions. Metals and Materials International, 2016, 22, 383-390.	1.8	11
482	Control of magnesium in vitro degradation based on ultrafine-grained surface gradient structure using ultrasonic nanocrystalline surface modification. Materialia, 2020, 12, 100821.	1.3	11
483	Effect of the Difference in Strength of Hard and Soft Components on the Synergetic Strengthening of Layered Materials. Metals and Materials International, 2021, 27, 376-383.	1.8	11
484	Enhanced thermoelectric performance of Bi0.5Sb1.5Te3 composites through potential barrier scattering at heterogeneous interfaces. Materials Research Bulletin, 2021, 133, 111023.	2.7	11
485	Evolution of microstructure and mechanical properties of [Cu–10Ni]–Si3N4 nanocomposites developed using mechanical alloying and spark plasma sintering. Journal of Alloys and Compounds, 2022, 899, 163319.	2.8	11
486	Cold Spray and Laser-Assisted Cold Spray of CrMnCoFeNi High Entropy Alloy Using Nitrogen as the Propelling Gas. Journal of Thermal Spray Technology, 2022, 31, 1129-1142.	1.6	11

#	Article	IF	CITATIONS
487	Interface characteristics and mechanical behavior of additively manufactured multi-material of stainless steel and Inconel. Materials Science & Engineering A: Structural Materials: Properties, Microstructure and Processing, 2022, 847, 143318.	2.6	11
488	Multi-scale investigation on local strain and damage evolution of Al1050/steel/Al1050 clad sheet. Journal of Materials Research and Technology, 2022, 20, 128-138.	2.6	11
489	Constitutive Model for Cold Compaction of Ceramic Powder. Journal of the American Ceramic Society, 2002, 85, 2137-2138.	1.9	10
490	(Bi,La)4Ti3O12 (BLT) thin films grown from nanocrystalline perovskite nuclei for ferroelectric memory devices. Applied Physics Letters, 2004, 85, 4118-4120.	1.5	10
491	Microforming of Bulk Metallic Glasses: Constitutive Modelling and Applications. Materials Transactions, 2004, 45, 1228-1232.	0.4	10
492	Incorporation and drift of hydrogen at low temperatures in ZnO. Applied Physics Letters, 2007, 90, 092116.	1.5	10
493	Modelling microstructure evolution towards ultrafine crystallinity produced by severe plastic deformation. Journal of Materials Science, 2007, 42, 9092-9096.	1.7	10
494	MECHANICAL-ACTIVATED PHASE FORMATION OF NiTi IN THE PRESENCE OF NANOPARTICLES. Nano, 2013, 08, 1350048.	0.5	10
495	Inhomogeneity Through Warm Equal Channel Angular Pressing. Journal of Materials Engineering and Performance, 2013, 22, 1666-1671.	1.2	10
496	Cyclic Seismic Testing of Composite Concrete-Filled U-Shaped Steel Beam to H-Shaped Column Connections. Journal of Structural Engineering, 2013, 139, 360-378.	1.7	10
497	Ga-doped indium oxide nanowire phase change random access memory cells. Nanotechnology, 2014, 25, 055205.	1.3	10
498	Al/C60 Nanocomposites Fabricated by High-Pressure Torsion. Metallurgical and Materials Transactions A: Physical Metallurgy and Materials Science, 2015, 46, 1838-1842.	1.1	10
499	Effect of surface etching on the tensile behavior of coarse- and ultrafine-grained pure titanium. Materials Science & Engineering A: Structural Materials: Properties, Microstructure and Processing, 2017, 707, 337-343.	2.6	10
500	Finite Element Analysis of Severe Plastic Deformation by Rectangular Vortex Extrusion. Metals and Materials International, 2021, 27, 676-682.	1.8	10
501	Printed Stretchable Single-Nanofiber Interconnections for Individually-Addressable Highly-Integrated Transparent Stretchable Field Effect Transistor Array. Nano Letters, 2021, 21, 5819-5827.	4.5	10
502	Temperature- and strain-dependent thermally-activated deformation mechanism of a ferrous medium-entropy alloy. Intermetallics, 2021, 134, 107202.	1.8	10
503	Development of the PC-GMAW welding technology for TMCP steel in accordance with welding thermal cycle, welding technique, structure, and properties of welded joints. Reports in Mechanical Engineering, 2020, 1, 26-33.	4.9	10
504	Determination of damage model parameters using nano- and bulk-scale digital image correlation and the finite element method. Journal of Materials Research and Technology, 2022, 17, 392-403.	2.6	10

#	Article	IF	CITATIONS
505	Origin of superior low-cycle fatigue resistance of an interstitial metastable high-entropy alloy. Journal of Materials Science and Technology, 2022, 115, 115-128.	5.6	10
506	Upgrading of superior strength–ductility trade-off of CoCrFeNiMn high-entropy alloy by microstructural engineering. Materialia, 2022, 22, 101394.	1.3	10
507	A precipitation-hardened AlSi10Mg alloy fabricated using selective laser melting. Materials Science & Engineering A: Structural Materials: Properties, Microstructure and Processing, 2022, 844, 143164.	2.6	10
508	Asymmetry evolutions in microstructure and strain hardening behavior between tension and compression for AZ31 magnesium alloy. Materials Science & Engineering A: Structural Materials: Properties, Microstructure and Processing, 2022, 844, 143168.	2.6	10
509	Bauschinger Effect or Kinematic Hardening: Bridging Microstructure and Continuum Mechanics. Metals and Materials International, 2023, 29, 280-292.	1.8	10
510	Deposition of CeO2 and NiO buffer layers for YBCO coated conductors on biaxially textured Ni substrates by a MOCVD technique. Physica C: Superconductivity and Its Applications, 2003, 386, 327-332.	0.6	9
511	Equal Channel Angular Pressing of Metallic Powders. Materials Science Forum, 2003, 437-438, 89-92.	0.3	9
512	Non-equilibrium Microstructure and Thermal Stability of Plasma-sprayed Al–Si Coatings. Journal of Materials Research, 2005, 20, 2038-2045.	1.2	9
513	Densification and Conolidation of Powders by Equal Channel Angular Pressing. Materials Science Forum, 2007, 534-536, 253-256.	0.3	9
514	Deformation Characteristics Evaluation of Modified Equal Channel Angular Pressing Processes. Materials Transactions, 2010, 51, 46-50.	0.4	9
515	Kinetic study of non-isothermal crystallization in Al80Fe10Ti5Ni5 metallic glass. Metals and Materials International, 2013, 19, 901-906.	1.8	9
516	Impact Toughness of Ultrafineâ€Grained Commercially Pure Titanium for Medical Application. Advanced Engineering Materials, 2018, 20, 1700863.	1.6	9
517	Welding Thermal Cycle Impact on the Microstructure and Mechanical Properties of Thermo–Mechanical Control Process Steels. Steel Research International, 2021, 92, 2000645.	1.0	9
518	Unraveling the discontinuous plastic flow of a Co-Cr-Fe-Ni-Mo multiprincipal-element alloy at deep cryogenic temperatures. Physical Review Materials, 2021, 5, .	0.9	9
519	Effect of heat treatment on microstructural heterogeneity and mechanical properties of 1%C-CoCrFeMnNi alloy fabricated by selective laser melting. Additive Manufacturing, 2021, 47, 102283.	1.7	9
520	Synergistic Effects of MWCNTs and High-Pressure Torsion-Induced Grain Refinement on Microhardness, Tribological Properties, and Corrosion Behavior of Cu and Cu/MWCNT Nanocomposites. Metals and Materials International, 2022, 28, 2197-2215.	1.8	9
521	Thermodynamic prediction of glass forming range in Al-Mg-REM ternary system. Calphad: Computer Coupling of Phase Diagrams and Thermochemistry, 1998, 22, 221-230.	0.7	8
522	Title is missing!. Journal of Materials Science Letters, 2002, 21, 353-355.	0.5	8

#	Article	IF	CITATIONS
523	Texture and surface analysis of NiO buffer deposited on biaxially textured Ni tapes by a MOCVD method. IEEE Transactions on Applied Superconductivity, 2003, 13, 2539-2542.	1.1	8
524	Prediction of the Forming Limit of Porous Metals Using the Finite Element Method. Materials Transactions, 2004, 45, 1829-1832.	0.4	8
525	Pulsed laser deposition of high-quality ZnO films using a high temperature deposited ZnO buffer layer. Applied Physics A: Materials Science and Processing, 2008, 91, 255-259.	1.1	8
526	Constitutive model for high temperature deformation behavior of Ti–Zr–Ni–Be bulk metallic glass in supercooled liquid region. Computational Materials Science, 2012, 61, 213-223.	1.4	8
527	Correlation of Microstructure with Mechanical Properties of Zr-Based Amorphous Matrix Composite Reinforced with Tungsten Continuous Fibers and Ductile Dendrites. Metallurgical and Materials Transactions A: Physical Metallurgy and Materials Science, 2012, 43, 4088-4096.	1.1	8
528	Plastic Deformation Behavior and Microstructural Evolution of Al-Core/Cu-Sheath Composites in Multi-pass Caliber Rolling. Metallurgical and Materials Transactions A: Physical Metallurgy and Materials Science, 2015, 46, 260-269.	1.1	8
529	Streamline approach to die design and investigation of material flow during the vortex extrusion process. Applied Mathematical Modelling, 2016, 40, 3550-3560.	2.2	8
530	Influence of high-pressure torsion and hot rolling on the microstructure and mechanical properties of aluminum–fullerene composites. Journal of Materials Science, 2017, 52, 11988-12000.	1.7	8
531	Influence of Friction Stir Processing Parameters on the Microstructure of Aluminum Foams. Transactions of the Indian Institute of Metals, 2018, 71, 483-491.	0.7	8
532	Circumferential twisting during route B equal-channel angular pressing. Journal of Materials Processing Technology, 2018, 259, 305-311.	3.1	8
533	Severe Plastic Deformation Methods for Bulk Samples. , 2018, , 37-112.		8
534	Physics-Based Constitutive Model of Porous Materials for Die/Isostatic Compaction of Metallic Powders. Metals and Materials International, 2020, 26, 221-229.	1.8	8
535	Biocompatible Magnesium Implant Double-Coated with Dexamethasone-Loaded Black Phosphorus and Poly(lactide- <i>co</i> -glycolide). ACS Applied Bio Materials, 2020, 3, 8879-8889.	2.3	8
536	Effect of Porosity on Mechanical Anisotropy of 316L Austenitic Stainless Steel Additively Manufactured by Selective Laser Melting. Journal of Korean Powder Metallurgy Institute, 2018, 25, 475-481.	0.2	8
537	Hierarchical heterostructured FeCr–(Mg–Mg2Ni) composite with 3D interconnected and lamellar structures synthesized by liquid metal dealloying. Journal of Materials Research and Technology, 2021, 15, 4573-4579.	2.6	8
538	Solid solution induced back-stress in multi-principal element alloys: Experiment and modeling. Materials Science & Engineering A: Structural Materials: Properties, Microstructure and Processing, 2022, 835, 142621.	2.6	8
539	Optimization of the pulsed arc welding parameters for wire arc additive manufacturing in austenitic steel applications. International Journal of Advanced Manufacturing Technology, 2022, 119, 5175-5193.	1.5	8
540	Modelling of Equal Channel Angular Pressing for Ultrafine-Grained Metals. Materials Science Forum, 2002, 386-388, 421-426.	0.3	7

#	Article	IF	CITATIONS
541	Fictive stress model based finite element analysis for bulk metallic glasses at an elevated temperature. Metals and Materials International, 2004, 10, 461-466.	1.8	7
542	Severe plastic deformation by the cone-cone method: potential for producing ultrafine grained sheet material. Revue De Metallurgie, 2007, 104, 318-322.	0.3	7
543	Plastic Flow and Strain Homogeneity of an Equal Channel Angular Pressing Process Enhanced through Forward Extrusion. Materials Transactions, 2010, 51, 977-981.	0.4	7
544	Shallow and Deep Centers in As-Grown and Annealed MgZnO/ZnO Structures with Quantum Wells. Journal of Electronic Materials, 2010, 39, 601-607.	1.0	7
545	Deformation behavior of consecutive workpieces in equal channel angular pressing of solid dies. Journal of Materials Science, 2012, 47, 7877-7882.	1.7	7
546	Local and Global Stress–Strain Behaviors of Transformation-Induced Plasticity Steel Using the Combined Nanoindentation and Finite Element Analysis Method. Metallurgical and Materials Transactions A: Physical Metallurgy and Materials Science, 2014, 45, 6008-6015.	1.1	7
547	Quasi-static and dynamic compressive properties of Ti-based amorphous alloys modified from conventional Ti–6Al–4V alloy. Materials Science & Engineering A: Structural Materials: Properties, Microstructure and Processing, 2014, 607, 197-205.	2.6	7
548	Novel strip-cast Mg/Al clad sheets with excellent tensile and interfacial bonding properties. Scientific Reports, 2016, 6, 26333.	1.6	7
549	Small-Scale System for Evaluation of Stretch-Flangeability with Excellent Reliability. Jom, 2018, 70, 912-917.	0.9	7
550	Development and Microstructural Characterization of a New Wrought High Entropy Superalloy. Metals and Materials International, 2020, 26, 591-602.	1.8	7
551	High Coercivity in MnAl Disc Prepared by Severe Plastic Deformation. Physica Status Solidi (B): Basic Research, 2020, 257, 1900356.	0.7	7
552	Superplastic Behavior in High-Pressure Torsion-Processed Mo7.5Fe55Co18Cr12.5Ni7 Medium-Entropy Alloy. Metallurgical and Materials Transactions A: Physical Metallurgy and Materials Science, 2021, 52, 1-7.	1.1	7
553	Stretch-flangeability of CoCrFeMnNi high-entropy alloy. Materials Science & Engineering A: Structural Materials: Properties, Microstructure and Processing, 2021, 814, 141241.	2.6	7
554	1.7 Gpa tensile strength in ferrous medium entropy alloy via martensite and precipitation. Materials Letters, 2022, 307, 130958.	1.3	7
555	Novel multi-metal stainless steel (316L)/high-modulus steel (Fe-TiB2) composite with enhanced specific modulus and strength using high-pressure torsion. Materials Letters, 2021, 303, 130510.	1.3	7
556	Analysis of texture and grain shape effects on the yield anisotropy of Zr-2.5wt%Nb pressure tube alloy using crystal plasticity finite element method. Journal of Nuclear Materials, 2021, 555, 153112.	1.3	7
557	Double-humped strain hardening in a metastable ferrous medium-entropy alloy by cryogenic pre-straining and subsequent heat treatment. Scripta Materialia, 2022, 211, 114511.	2.6	7
558	Importance of Microstructural Features in Bimodal Structure–Property Linkage. Metals and Materials International, 2023, 29, 53-58.	1.8	7

#	Article	IF	CITATIONS
559	Determining reliable wide-strain-range equivalent stress–strain curves using 3D digital image correlation. Journal of Materials Research and Technology, 2022, 19, 2822-2830.	2.6	7
560	Title is missing!. Journal of Materials Science, 2001, 36, 5881-5884.	1.7	6
561	Deformation behavior of strip-cast bulk amorphous matrix composites containing various crystalline particles. Materials Science & Engineering A: Structural Materials: Properties, Microstructure and Processing, 2007, 449-451, 176-180.	2.6	6
562	Predicting the Adiabatic Temperature of Transparent Y ₃ Al ₅ O ₁₂ Prepared via Combustion Synthesis under Ultra-High Gravity. Materials Transactions, 2010, 51, 2230-2235.	0.4	6
563	Comparison of deformation and microstructural evolution between equal channel angular pressing and forward extrusion using the dislocation cell mechanism-based finite element method. Journal of Materials Science, 2010, 45, 4705-4710.	1.7	6
564	Adiabatic Shear Banding in an Al-Mg-Si Alloy Processed by Equal Channel Angular Pressing. Materials Science Forum, 2010, 654-656, 1014-1017.	0.3	6
565	Effect of Homogenization Treatment on the Microstructure and Mechanical Property Evolutions of As-Cast Al–Cu Alloy during High-Pressure Torsion. Materials Transactions, 2014, 55, 1405-1413.	0.4	6
566	Strain Softening Induced by High Pressure Torsion in Copper Alloys. Materials Transactions, 2015, 56, 1658-1663.	0.4	6
567	Dynamic tensile deformation behavior of Zr-based amorphous alloy matrix composites reinforced with tungsten or tantalum fibers. Metals and Materials International, 2016, 22, 707-713.	1.8	6
568	Effects of dendrite size on dynamic tensile deformation behavior in Zr-based amorphous alloys containing ductile dendrites. Materials Science & Engineering A: Structural Materials: Properties, Microstructure and Processing, 2016, 650, 102-109.	2.6	6
569	Development of Methodology with Excellent Reproducibility for Evaluating Stretch-Flangeability Using a Sheared-Edge Tensile Test. Experimental Mechanics, 2017, 57, 1349-1358.	1.1	6
570	Simulation of Pipe-Manufacturing Processes Using Sheet Bending-Flattening. Experimental Mechanics, 2018, 58, 909-918.	1.1	6
571	Data to reproduce and modify "An approach for screening single phase high-entropy alloys using an in-house thermodynamic database― Data in Brief, 2018, 20, 1337-1339.	0.5	6
572	Yield-strength prediction of flattened steel pipes by competing Bauschinger effect and strain hardening during pipe-forming. Scientific Reports, 2019, 9, 14002.	1.6	6
573	Grain Size Effect on Mechanical Properties Under Biaxial Stretching in Pure Tantalum. Metals and Materials International, 2019, 25, 1448-1456.	1.8	6
574	On the control of structural/compositional ratio of coherent order-disorder interfaces. Journal of Alloys and Compounds, 2019, 777, 1222-1233.	2.8	6
575	A novel approach for producing <i>in situ</i> Al-Al ₂ Cu composite via friction stir processing. Materials Research Express, 2019, 6, 036528.	0.8	6
576	A thermodynamic description of the Al–Cu–Fe–Mn system for an immiscible medium-entropy alloy design. Calphad: Computer Coupling of Phase Diagrams and Thermochemistry, 2020, 71, 101995.	0.7	6

#	Article	IF	CITATIONS
577	Effect of Processing Route on Microstructure and Mechanical Properties in Single-Roll Angular-Rolling. Materials, 2020, 13, 2471.	1.3	6
578	Ultrafine Grained Cu-diamond Composites using High Pressure Torsion. Journal of Korean Powder Metallurgy Institute, 2012, 19, 204-209.	0.2	6
579	An Effective Strengthening Strategy of Nano Carbide Precipitation and Cellular Microstructure Refinement in a Superalloy Fabricated by Selective Laser Melting Process. Metals, 2021, 11, 1691.	1.0	6
580	Novel deep learning approach for practical applications of indentation. Materials Today Advances, 2022, 13, 100207.	2.5	6
581	Constitutive modeling and finite element analysis of metastable medium entropy alloy. Materials Science & Engineering A: Structural Materials: Properties, Microstructure and Processing, 2022, 840, 142915.	2.6	6
582	Mechanical and magnetic properties of soft magnetic Fe–Ni permalloy produced by directed energy deposition processes. Journal of Materials Science, 2022, 57, 17967-17983.	1.7	6
583	Grain Refinement and Texture Evolution in AZ31 Alloy during ECAP Process and Their Effects on Mechanical Properties. Materials Science Forum, 2005, 475-479, 549-554.	0.3	5
584	Analyses of route Bc equal channel angular pressing and post-equal channel angular pressing behavior by the finite element method. Journal of Materials Science, 2010, 45, 4682-4688.	1.7	5
585	Analysis and estimation of yield strength of API X80 linepipe steel pipe by low-cycle fatigue tests. Metals and Materials International, 2012, 18, 597-606.	1.8	5
586	Design of Hierarchical Cellular Metals Using Accumulative Bundle Extrusion. Metallurgical and Materials Transactions A: Physical Metallurgy and Materials Science, 2013, 44, 4031-4036.	1.1	5
587	Dendrite size and tensile ductility in Ti-based amorphous alloys containing ductile dendrites. Materials Science & Engineering A: Structural Materials: Properties, Microstructure and Processing, 2013, 587, 143-149.	2.6	5
588	Finite Element Simulation of Powder Compaction via Shock Consolidation Using Gas-gun System. Procedia Engineering, 2014, 81, 1180-1185.	1.2	5
589	Effects of Effective Dendrite Size on Dynamic Tensile Properties of Ti-Based Amorphous Matrix Composites. Metallurgical and Materials Transactions A: Physical Metallurgy and Materials Science, 2016, 47, 1504-1509.	1.1	5
590	Online Measurement of Electrospinning Jet Velocity of Polyvinyl Alcohol. International Polymer Processing, 2016, 31, 285-291.	0.3	5
591	Wear Resistance of the La62Cu12Ni12Al14 Bulk Metallic Glass Under Dry Friction Conditions. Tribology Letters, 2017, 65, 1.	1.2	5
592	Stretch-flangeability of twinning-induced plasticity steel-cored three-layer steel sheet. Journal of Materials Processing Technology, 2018, 258, 220-225.	3.1	5
593	Applications of Ultrafine-Grained and Nanograined Metals. , 2018, , 275-306.		5
594	Quantitative study on yield point phenomenon of low carbon steels processed by compact endless casting and rolling. Materials Science & Engineering A: Structural Materials: Properties, Microstructure and Processing, 2018, 734, 408-415.	2.6	5

#	Article	IF	CITATIONS
595	Understanding and Avoiding Intergranular Fracture Characteristics of Hadfield/Hot-Press-Forming Multi-Layer Steel Sheets. Metallurgical and Materials Transactions A: Physical Metallurgy and Materials Science, 2019, 50, 4085-4097.	1.1	5
596	Diffuse γ/γ′ interfaces in the hierarchical dual-phase nanostructure of a Ni-Al-Ti alloy. Materials Characterization, 2019, 153, 284-293.	1.9	5
597	Analysis of bending behavior of TiN particle-reinforced martensitic steel using micro-digital image correlation. Materials Science & Engineering A: Structural Materials: Properties, Microstructure and Processing, 2020, 794, 139965.	2.6	5
598	On the mechanistic understanding of annealing-induced strength enhancement of ultrafine-grained high-Mn steel. Materialia, 2020, 13, 100837.	1.3	5
599	The role of ultrasonic nanocrystalline surface modification at elevated temperature on the hydrogen charging behavior of high-Mn steels. Materialia, 2020, 9, 100626.	1.3	5
600	Effects of temperature and loading rate on phase stability and deformation mechanism in metastable V10Cr10Co30FexNi50-x high entropy alloys. Materials Science & Engineering A: Structural Materials: Properties, Microstructure and Processing, 2021, 804, 140766.	2.6	5
601	Excellent strength-ductility combination of multi-layered sheets composed of high-strength V10Cr10Fe50Co30 high entropy alloy and 304 austenitic stainless steel. Materials Science & Engineering A: Structural Materials: Properties, Microstructure and Processing, 2021, 823, 141727.	2.6	5
602	Microstructural evolution of equal-channel angular pressed interstitial-free steel. International Journal of Materials Research, 2009, 100, 834-837.	0.1	5
603	Densification and Nanocrystallization of Water-Atomized Pure Iron Powder Using High Pressure Torsion. Journal of Korean Powder Metallurgy Institute, 2011, 18, 411-416.	0.2	5
604	Ultrafine Grained Bulk Al Matrix Carbon Nanotube Composites Processed by High Pressure Torsion. Transactions of Materials Processing, 2010, 19, 423-428.	0.1	5
605	Effects of constrained groove pressing on mechanical properties of a TWIP steel. Materials Science and Technology, 2021, 37, 1291-1301.	0.8	5
606	Mechanical properties and microstructural evolution of high-pressure torsion-processed Al7075 alloy at elevated temperatures. Materials Science & Engineering A: Structural Materials: Properties, Microstructure and Processing, 2022, 835, 142692.	2.6	5
607	Role of cellular structure on deformation twinning and hetero-deformation induced strengthening of laser powder-bed fusion processed CuSn alloy. Additive Manufacturing, 2022, 54, 102744.	1.7	5
608	Excellent combination of cryogenic strength and ductility of a metastable Fe65Ni15Co8Mn8Ti3Si medium entropy alloy through the exceptional deformation-induced martensitic transformation. Journal of Materials Science, 2022, 57, 18062-18074.	1.7	5
609	Massâ€Transfer Effects on the Anodic Behavior of Porous Fe and Co Sintered Electrodes in Aqueous Ammoniacal Solution. Journal of the Electrochemical Society, 1991, 138, 1599-1607.	1.3	4
610	Multi-Scale Modelling Scheme for Carbon Nanotube Reinforced Metal Matrix Composites. Key Engineering Materials, 2007, 345-346, 1261-1264.	0.4	4
611	Mechanical behavior and microstructure of Cu54Zr22Ti18Ni6 bulk metallic glass at elevated temperatures. Materials Science & Engineering A: Structural Materials: Properties, Microstructure and Processing, 2007, 449-451, 122-125.	2.6	4
612	Yield and Densification Behavior of Rapidly Solidified Magnesium Powders. Materials Transactions, 2008, 49, 967-971.	0.4	4

#	Article	IF	CITATIONS
613	Plastic deformation analysis of accumulative back extrusion. International Journal of Materials Research, 2009, 100, 1715-1719.	0.1	4
614	A New Technique for Severe Plastic Deformation: The Cone–Cone Method. Advanced Engineering Materials, 2009, 11, 982-985.	1.6	4
615	Consolidation of Amorphous Powders by Hot Pressing. Journal of Nanomaterials, 2012, 2012, 1-10.	1.5	4
616	Microstructure and Thermal Stability of Copper - Carbon Nanotube Composites Consolidated by High Pressure Torsion. Materials Science Forum, 2012, 729, 228-233.	0.3	4
617	Finite Element Analysis of Deformation Homogeneity During Continuous and Batch Type Equal Channel Angular Pressing. Journal of Materials Engineering and Performance, 2013, 22, 3222-3227.	1.2	4
618	Anisotropy of Dynamic Compressive Properties of Non-Heat-Treating Cold-Heading-Quality Steel Bars. Metallurgical and Materials Transactions A: Physical Metallurgy and Materials Science, 2014, 45, 1294-1305.	1.1	4
619	Investigation of thermal resistance and power consumption in Ga-doped indium oxide (In ₂ O ₃) nanowire phase change random access memory. Applied Physics Letters, 2014, 104, 103510.	1.5	4
620	Circumferential shear strain in torsion-based severe plastic deformation. Scripta Materialia, 2014, 82, 41-44.	2.6	4
621	Unique Appearance of Lamellar Cleavage Patterns on Fracture Surfaces of Ti-Based Amorphous Matrix Composite. Metallurgical and Materials Transactions A: Physical Metallurgy and Materials Science, 2015, 46, 2506-2515.	1.1	4
622	Simulation of the Effective of Friction on the Deformation in Equal Channel Angular Pressing (ECAP). Key Engineering Materials, 0, 656-657, 526-531.	0.4	4
623	Bi-modal Structure of Copper via Room-Temperature Partial Recrystallization After Cryogenic Dynamic Compression. Metallurgical and Materials Transactions A: Physical Metallurgy and Materials Science, 2016, 47, 1600-1606.	1.1	4
624	Microstructure and Mechanical Properties of Al-3 Vol% CNT Nanocomposites Processed by High-Pressure Torsion. Archives of Metallurgy and Materials, 2017, 62, 1109-1112.	0.6	4
625	Stretchability and drawability of twinning-Induced plasticity steel-Cored layer steel sheets. Journal of Materials Processing Technology, 2017, 250, 357-362.	3.1	4
626	Mechanical Properties of Ultrafine-Grained and Nanostructured Metals. , 2018, , 223-257.		4
627	Effective Parameters for the Success of Severe Plastic Deformation Methods. , 2018, , 187-222.		4
628	Severe Plastic Deformation for Industrial Applications. , 2018, , 165-186.		4
629	Solid state recycling of aluminium AA6061 alloy chips by hot extrusion. Materials Research Express, 2019, 6, 036525.	0.8	4
630	Modelling feasibility constraints for materials design: Application to inverse crystallographic texture problem. Computational Materials Science, 2019, 156, 361-367.	1.4	4

#	Article	IF	CITATIONS
631	Effect of multi-pass friction stir processing on the microstructure and hardness of AA1100/Al13Fe4 in situ composites. Materials Research Express, 2019, 6, 046558.	0.8	4
632	Continuous Severe Plastic Deformation of Lowâ€Carbon Steel: Physical–Mechanical Properties and Multiscale Structure Analysis. Steel Research International, 2021, 92, 2000482.	1.0	4
633	Strength–ductility enhancement in multi-layered sheet with high-entropy alloy and high-Mn twinning-induced plasticity steel. Materials Science & Engineering A: Structural Materials: Properties, Microstructure and Processing, 2021, 822, 141670.	2.6	4
634	Metastable δ-ferrite and twinning-induced plasticity on the strain hardening behavior of directed energy deposition-processed 304L austenitic stainless steel. Additive Manufacturing, 2021, 47, 102363.	1.7	4
635	Correlation Between Superheated Liquid Fragility And Onset Temperature Of Crystallization For Al-Based Amorphous Alloys. Archives of Metallurgy and Materials, 2015, 60, 1543-1546.	0.6	4
636	Effects of Friction and Anvil Design on Plastic Deformation during the Compression Stage of High-Pressure Torsion. Journal of Korean Institute of Metals and Materials, 2016, 54, 831-837.	0.4	4
637	Inhomogeneous Hardness Distribution of High Pressure Torsion Processed IF Steel Disks. Materials Sciences and Applications, 2012, 03, 234-239.	0.3	4
638	Consolidation and Mechanical Behavior of Gas Atomized MgZn _{4.3} Y _{0.7} Alloy Powders using High Pressure Torsion. Journal of Korean Powder Metallurgy Institute, 2010, 17, 190-196.	0.2	4
639	Evolution of nanosized Cu-rich clusters in a Fe–15Cu–15Ni alloy produced by laser powder bed fusion. Materials Science & Engineering A: Structural Materials: Properties, Microstructure and Processing, 2022, 832, 142462.	2.6	4
640	Enhancement of tensile strength in AA 6061-T6 plates joined by gas tungsten arc welding using high entropy alloy filler sheet. Materials Science & Engineering A: Structural Materials: Properties, Microstructure and Processing, 2022, 832, 142481.	2.6	4
641	Strength and Fracture of Cu-Based Filamentary Nanocomposites. Key Engineering Materials, 2000, 183-187, 1207-1212.	0.4	3
642	Strength and Ductility of Ultrafine Grained Copper: Modelling and Experiment. Journal of Metastable and Nanocrystalline Materials, 2003, 17, 29-36.	0.1	3
643	Effect of μm-ZrC Dispersoids and Nanoprecipitates on Mechanical Properties of CuZrTi Bulk Glasses. Journal of Metastable and Nanocrystalline Materials, 2003, 15-16, 161-166.	0.1	3
644	Mechanical Modelling of Carbon Nanotube Reinforced Metal Matrix Composites. Journal of Metastable and Nanocrystalline Materials, 2005, 24-25, 383-386.	0.1	3
645	Simulation of Equal-Channel Angular Extrusion Pressing. Materials Science Forum, 2006, 503-504, 201-208.	0.3	3
646	Corrosion and Mechanical Behaviors of Cu-35%Zn Alloy Prepared by Equal Channel Angular Pressing (ECAP). Materials Science Forum, 2006, 503-504, 823-828.	0.3	3
647	Achieving Both Powder Consolidation and Grain Refinement for Bulk Nanostructured Materials by Equal-Channel Angular Pressing. Key Engineering Materials, 2007, 345-346, 173-176.	0.4	3
648	Molecular Dynamics Investigation on Microstructure and Void in Amorphous SiO ₂ . Materials Transactions, 2008, 49, 1212-1218.	0.4	3

#	Article	IF	CITATIONS
649	Microstructure evolution in ultrafine-grained interstitial free steel processed by high pressure torsion. IOP Conference Series: Materials Science and Engineering, 2014, 63, 012055.	0.3	3
650	Effect of Post-annealing on Grain Boundary of Nano-crystalline Cu Processed by Powder High-Pressure Torsion. Metallurgical and Materials Transactions A: Physical Metallurgy and Materials Science, 2014, 45, 4748-4752.	1.1	3
651	Finite Element Analysis for Application to the Forming Process of Ti-based Bulk Metallic Glasses. Materials and Manufacturing Processes, 2014, 29, 801-807.	2.7	3
652	Role of an encapsulating layer for reducing resistance drift in phase change random access memory. AIP Advances, 2014, 4, .	0.6	3
653	Electron Holography: Correlative Highâ€Resolution Mapping of Strain and Charge Density in a Strained Piezoelectric Multilayer (Adv. Mater. Interfaces 1/2015). Advanced Materials Interfaces, 2015, 2, .	1.9	3
654	Effect of friction stir processing on the microstructure of pure magnesium castings. International Journal of Cast Metals Research, 2015, 28, 345-351.	0.5	3
655	Interpretation of Fracture Toughness and R-Curve Behavior by Direct Observation of Microfracture Process in Ti-Based Dendrite-Containing Amorphous Alloys. Metallurgical and Materials Transactions A: Physical Metallurgy and Materials Science, 2015, 46, 1588-1596.	1.1	3
656	Ring-Constraint High-Pressure Torsion Process. Metallurgical and Materials Transactions A: Physical Metallurgy and Materials Science, 2016, 47, 3473-3478.	1.1	3
657	Compressibility of hierarchic-architectured agglomerates of hydrogen-reduced copper nanopowders. Journal of Materials Science, 2016, 51, 82-95.	1.7	3
658	Finite Element and Experimental Analyses on the Formability of Steel Sheets Produced by Compact Endless Cast and Rolling. Metallurgical and Materials Transactions A: Physical Metallurgy and Materials Science, 2017, 48, 1021-1032.	1.1	3
659	Influences of high strain rate, low temperature, and deformation direction on microstructural evolution and mechanical properties of copper. Materials Science & Engineering A: Structural Materials: Properties, Microstructure and Processing, 2017, 684, 567-576.	2.6	3
660	Deep drawing behavior of twinning-induced plasticity-cored three-layer steel sheet. International Journal of Material Forming, 2018, 11, 11-18.	0.9	3
661	Severe Plastic Deformation Methods for Tubular Samples. , 2018, , 131-164.		3
662	Effect of Highâ€Pressure Torsion on the Thermal and Mechanical Properties of La 62 Cu 12 Ni 12 Al 14 Bulk Metallic Glass. Advanced Engineering Materials, 2019, 21, 1800918.	1.6	3
663	Microstructure, Microâ€Hardness, and Corrosion Resistance of Commercial Purity Al Processed by Hollow one Highâ€Pressure Torsion. Advanced Engineering Materials, 2019, 21, 1800905.	1.6	3
664	INDENTATION SIZE EFFECT IN HIGH PRESSURE TORSION PROCESSED HIGH ENTROPY ALLOY. Acta Polytechnica CTU Proceedings, 0, 27, 141-144.	0.3	3
665	Microstructural and Mechanical Properties of a Material Processed by Streamline Proposed Vortex Extrusion Die. Metals and Materials International, 2021, 27, 522-529.	1.8	3
666	Consolidation and Mechanical Property of Rapidly Solidified Al-20 wt% Si Alloy Powders by Continuous Equal Channel Multi-Angular Pressing. Journal of Korean Powder Metallurgy Institute, 2008, 15, 31-36.	0.2	3

#	Article	IF	CITATIONS
667	Effect of Particle Size on Compactibility of Water-atomized Pure Iron Powder. Journal of Korean Powder Metallurgy Institute, 2011, 18, 221-225.	0.2	3
668	Modeling of deformation behavior of copper under equal channel angular pressing. International Journal of Materials Research, 2022, 94, 754-760.	0.1	3
669	A New Digital Image Correlation Method for Measuring Wide Strain Range True Stress–Strain Curve of Clad Materials. Metals and Materials International, 2023, 29, 168-173.	1.8	3
670	Growth mode in strained ZnO films on Al2O3(0001) during sputtering. Journal of Electroceramics, 2006, 17, 327-330.	0.8	2
671	Processing of Ultrafine-Grained Cu-Fe-Cr Composite by Equal Channel Angular Pressing. Materials Science Forum, 2006, 503-504, 71-76.	0.3	2
672	Biomimetic Deposition of Apatite on Zr-1Nb and Ti-6Al-4V. Materials Science Forum, 2007, 534-536, 1013-1016.	0.3	2
673	Investigation of electrical and optical properties of ZnO thin films grown with O2/O3 gas mixture. Applied Physics A: Materials Science and Processing, 2008, 91, 251-254.	1.1	2
674	Acceptor state formation in arsenicâ€doped ZnO films grown using ozone. Physica Status Solidi (A) Applications and Materials Science, 2008, 205, 1647-1652.	0.8	2
675	MULTI-SCALE FINITE ELEMENT SIMULATION OF SEVERE PLASTIC DEFORMATION. International Journal of Modern Physics B, 2009, 23, 1621-1626.	1.0	2
676	Persistent photoconductivity in MgZnO alloys. Semiconductors, 2009, 43, 577-580.	0.2	2
677	Preface to the special issue on ultrafine-grained materials. Journal of Materials Science, 2012, 47, 7717-7718.	1.7	2
678	An electron back-scattered diffraction study on the microstructure evolution of severely deformed aluminum Al6061 alloy. IOP Conference Series: Materials Science and Engineering, 2014, 63, 012089.	0.3	2
679	Fabrication of W-Cu alloy via combustion synthesis infiltration under an ultra-gravity field. Metals and Materials International, 2014, 20, 1145-1150.	1.8	2
680	Strain induced hardening and softening behaviors of deformed Cu and Cu–Ge alloys. Journal of Materials Research, 2016, 31, 599-608.	1.2	2
681	Strain hardening and micro-deformation behavior in advanced DP and TRIP steels: EBSD examinations and crystal plasticity simulations. Materials Research Express, 2018, 5, 126507.	0.8	2
682	Microstructural and Finite Element Analysis of Creep Failure in Dissimilar Weldment Between 9Cr and 2.25Cr Heat-Resistant Steels. Metallurgical and Materials Transactions A: Physical Metallurgy and Materials Science, 2018, 49, 5323-5332.	1.1	2
683	Quantification of Mechanical Twins in Metallographic Images of Twinning-Induced Plasticity Steels Using a New Image Processing Method. Metals and Materials International, 2021, 27, 618-628.	1.8	2
684	Densification Behaviour of Magnesium Powders during Cold Isostatic Pressing using the Finite Element Method. Journal of Korean Powder Metallurgy Institute, 2007, 14, 362-366.	0.2	2

#	Article	IF	CITATIONS
685	Densification of Copper Powders using High-pressure Torsion Process. Journal of Korean Powder Metallurgy Institute, 2012, 19, 333-337.	0.2	2
686	Tomography-based Finite Element Analysis for the Mechanical Behavior of Porous Titanium Manufactured by a Space Holder Method. Journal of Korean Powder Metallurgy Institute, 2013, 20, 350-354.	0.2	2
687	Planar Shock Wave Compaction of Oxidized Copper Nano Powders using High Speed Collision and Its Mechanical Properties. Journal of Korean Powder Metallurgy Institute, 2014, 21, 39-43.	0.2	2
688	Quantitative Analysis of Roughness of Powder Surface Using Three-Dimensional Laser Profiler and its Effect on Green Strength of Powder Compacts. Journal of Korean Powder Metallurgy Institute, 2011, 18, 406-410.	0.2	2
689	Nanoporous Materials: Beating Thermal Coarsening in Nanoporous Materials via Highâ€Entropy Design (Adv. Mater. 6/2020). Advanced Materials, 2020, 32, 2070044.	11.1	2
690	A New Proposal for a Method to Measure Orthogonal R-Value Using a Single Tensile Test with Three-Dimensional Digital Image Correlation. Experimental Mechanics, 2022, 62, 999-1006.	1.1	2
691	AlCoCrFeNi-NiTi high entropy alloy composites: Microstructure and wear performance. Materials Today Communications, 2022, 32, 103952.	0.9	2
692	Experimental and numerical analyses of indentation in single piece and split type specimens. Journal of Materials Science, 2002, 37, 29-34.	1.7	1
693	Finite Element Analysis of Equal Channel Angular Pressing Based on a Dislocation Density and Cell Size Evolution Model. Journal of Metastable and Nanocrystalline Materials, 2003, 15-16, 231-234.	0.1	1
694	Phase Mixture Models for Metallic Materials with Submicrometer Grain Size. Materials Research Society Symposia Proceedings, 2003, 791, 1.	0.1	1
695	Creep Analysis of Cr-Mo Steels Using a Dislocation Based Constitutive Modelling. Materials Science Forum, 2004, 449-452, 117-120.	0.3	1
696	Modeling of Deformation Behavior and Texture Development in Aluminium under Equal Channel Angular Pressing. , 2005, , 233-238.		1
697	Three Dimensional Numerical Investigation of Equal Channel Multi-Angular Pressing. Materials Science Forum, 2006, 503-504, 931-936.	0.3	1
698	Biocompatibility and Mechanical Performance of Ni-Ti. Materials Science Forum, 2007, 534-536, 1617-1620.	0.3	1
699	Deformation Mechanism Map of Nanocrystalline Metallic Materials. Materials Science Forum, 2007, 539-543, 2816-2821.	0.3	1
700	Processing Conditions and Mechanical Properties of Fine Grained Mg by Equal Channel Angular Pressing. Key Engineering Materials, 2007, 340-341, 913-917.	0.4	1
701	Hot Workability of Ultrafine-Grained Aluminum Alloy Produced by Severe Plastic Deformation of Al6063 Powder and Consolidation. Materials Science Forum, 0, 667-669, 979-984.	0.3	1
702	Microstructural Aspects during the Preparation of Y ₃ Al ₅ O ₁₂ by Combustion Synthesis and Temperature Field Simulation. Materials Transactions, 2011, 52, 685-690.	0.4	1

#	Article	IF	CITATIONS
703	Metastable Phases in Al ₈₀ Fe ₁₀ Ti ₅ Ni ₅ Alloy Fabricated by Non-Equilibrium Processes. Materials Transactions, 2012, 53, 1739-1743.	0.4	1
704	Evaluation of Mechanical Properties of Tubular Materials With Hydraulic Bulge Test for Superconducting Radio Frequency (SRF) Cavities. IEEE Transactions on Applied Superconductivity, 2013, 23, 3500604-3500604.	1.1	1
705	Effect of Fiber Diameter on Quasi-static and Dynamic Compressive Properties of Zr-Based Amorphous Matrix Composites Reinforced with Stainless Steel Continuous Fibers. Metallurgical and Materials Transactions A: Physical Metallurgy and Materials Science, 2014, 45, 1284-1293.	1.1	1
706	Ultrafine-Grained Materials Fabrication with High Pressure Torsion and Simulation of Plastic Deformation Inhomogeneous Characteristics. , 2017, , .		1
707	Nanocrystalline High Entropy Alloys: Processing and Properties. , 2022, , 372-380.		1
708	Correlation with the composition of the different parts of p-type Bi0.5Sb1.5Te3 sintered bulks and their thermoelectric characteristics. Journal of Alloys and Compounds, 2020, 845, 156114.	2.8	1
709	Effect of Initial Grain Size on Deformation Mechanism during Highâ€Pressure Torsion in V ₁₀ Cr ₁₅ Mn ₅ Fe ₃₅ Co ₁₀ Ni ₂₅ Highâ€Entropy Alloy. Advanced Engineering Materials, 2020, 22, 2070002.	1.6	1
710	Finite Element Analysis on the Effect of Die Corner Angle in Equal Channel Angular Pressing Process of Powders. Journal of Korean Powder Metallurgy Institute, 2007, 14, 26-31.	0.2	1
711	Fabrication of Layered Cu-Fe-Cu Structure by Cold Consolidation of Powders using High-pressure Torsion. Journal of Korean Powder Metallurgy Institute, 2021, 28, 287-292.	0.2	1
712	Analysis of Densification Behavior during Powder Equal Channel Angular Pressing using Critical Relative Density Model. Journal of Korean Powder Metallurgy Institute, 2008, 15, 365-370.	0.2	1
713	Finite Element Analysis of the R-value of a 2-Layer Clad Steel. Transactions of Materials Processing, 2014, 23, 311-316.	0.1	1
714	Deformation lagging characteristics of IF steel disks in the plastic deformation process of high pressure torsion. Zhongguo Kexue Jishu Kexue/Scientia Sinica Technologica, 2018, 48, 154-160.	0.3	1
715	Fabrication of FeCuNi alloy by mechanical alloying followed by consolidation using high-pressure torsion. Journal of Korean Powder Metallurgy Institute, 2020, 27, 1-7.	0.2	1
716	The influence of laser powder-bed fusion microstructures on the corrosion behavior of CuSn alloy. Journal of Materials Science, 0, , 1.	1.7	1
717	Transformation-induced plasticity in the heterogeneous microstructured Ti-Zr-Nb-Sn alloy via in-situ alloying with directed energy deposition. Additive Manufacturing, 2022, 58, 102990.	1.7	1
718	Analysis of Deformation of Porous Metals. Materials Research Society Symposia Proceedings, 1998, 521, 33.	0.1	0
719	On the Modelling of Ultra-Fine Grained Materials. Journal of Metastable and Nanocrystalline Materials, 1999, 2-6, 437-442.	0.1	0
720	A Model on the Strengthening and Embrittlement of Devitrified Nanocomposites. Key Engineering Materials, 2000, 183-187, 1255-1260.	0.4	0

#	Article	IF	CITATIONS
721	Microstructural Evolution and Mechanical Flow of 6061 Al during Equal Channel Angular Pressing. Materials Science Forum, 2002, 386-388, 577-582.	0.3	0
722	Strengthening Mechanism of Zr-Based Devitrified Amorphous Nanocomposites with Quasicrystalline Phases. Journal of Metastable and Nanocrystalline Materials, 2003, 15-16, 205-208.	0.1	0
723	Modelling Mechanical Properties of Nanocrystalline Copper. Materials Science Forum, 2003, 437-438, 351-354.	0.3	0
724	Analysis of the Tensile Deformation Behaviour of Nanocrystalline Metals - A Multi-Scale Approach. Journal of Metastable and Nanocrystalline Materials, 2003, 15-16, 227-230.	0.1	0
725	Influence of <i>In-Situ</i> Nanoprecipitation on Constant Load Deformation in the Class Transition Region of a Cu ₆₀ Zr ₃₀ Ti ₁₀ Bulk Metallic Class. Materials Transactions, 2004, 45, 2383-2388.	0.4	0
726	Process Modeling of Equal Channel Angular Pressing. , 2005, , 239-244.		0
727	Superplastic Behavior of Deformation Processed Cu-Ag Nanocomposites. , 2005, , 728-733.		0
728	Deformation Mechanisms of Nanostructured Metallic Materials. Journal of Metastable and Nanocrystalline Materials, 2005, 24-25, 709-714.	0.1	0
729	Analytical and Numerical Modelling of Strain and Strain Rate in Equal Channel Angular Pressing (ECAP). Key Engineering Materials, 2006, 306-308, 965-970.	0.4	0
730	Strength of Nanostructured Materials Using a Phase Mixture Model. Key Engineering Materials, 2006, 306-308, 1085-1090.	0.4	0
731	Properties of postâ€annealed ZnO films grown with O ₃ . Physica Status Solidi (A) Applications and Materials Science, 2008, 205, 1631-1635.	0.8	0
732	Reply to the comments of article—On the effect of acute angles on deformation homogeneity in equal channel angular pressing. Materials Science & Engineering A: Structural Materials: Properties, Microstructure and Processing, 2008, 472, 358-359.	2.6	0
733	Finite Element Investigation of the Effect of Hardening Behavior of Alloys on Equal Channel Angular Pressing Performance. Materials Science Forum, 2008, 584-586, 1021-1026.	0.3	0
734	Thermal Stability, Microstructure and Mechanical Properties of Nanostructured Al-Ni-Mm-X (X = Cu) Tj ETQq0 0 C) rgBT /Ove	erlgck 10 Tf 5
735	Quantum Dots: Bandgap Tuning with Thermal Residual Stresses Induced in a Quantum Dot (Small) Tj ETQq1 1 0.	784314 rg	gBT /Overla <mark>c</mark> t
736	Microstructure and Defect Structure Evolution in Ultra-Fine Grained MgAlZn Alloy. Materials Science Forum, 0, 783-786, 390-395.	0.3	0
737	Effect of target-fixture geometry on shock-wave compacted copper powders. Metals and Materials International, 2018, 24, 84-94.	1.8	0
738	Force Sensors: A Highly Sensitive Force Sensor with Fast Response Based on Interlocked Arrays of Indium Tin Oxide Nanosprings toward Human Tactile Perception (Adv. Funct. Mater. 42/2018). Advanced Functional Materials, 2018, 28, 1870304.	7.8	0

#	Article	IF	CITATIONS
739	Surface Abrasive Torsion for Improved Mechanical Properties and Microstructure. Metallurgical and Materials Transactions A: Physical Metallurgy and Materials Science, 2018, 49, 3151-3156.	1.1	0
740	Mechanical Properties of a Cu55Zr30Ti10Pd5Bulk Amorphous Alloy. Korean Journal of Materials Research, 2005, 15, 281-284.	0.1	0
741	Analysis of Aluminum Powder Densification by Continuous Front Extrusion-Equal Channel Angular Pressing. Journal of Korean Powder Metallurgy Institute, 2008, 15, 204-209.	0.2	0
742	Analysis of Densification Behavior of Magnesium Powders in Extrusion using the Critical Relative Density Model. Journal of Korean Powder Metallurgy Institute, 2009, 16, 50-55.	0.2	0
743	Finite Element Analysis of Densification of Mg Powders during Equal Channel Angular Pressing: Effect of Sheath. Journal of Korean Powder Metallurgy Institute, 2009, 16, 85-90.	0.2	0
744	Investigation of Microhardness and Microstructure of AZ31 Alloy after High Pressure Torsion. , 2011, , 589-594.		0
745	Fabrication of Silicon Carbide Quantum Dots via Chemical-Etching Approach and Fluorescent Imaging for Living Cells. Materials Sciences and Applications, 2014, 05, 177-182.	0.3	0
746	Manufacturing and Evaluation of the Properties of Hybrid Bulk Material by Shock-compaction of Nanocrystalline Cu-Ni Mixed Powder. Journal of Korean Powder Metallurgy Institute, 2014, 21, 196-201.	0.2	0
747	Analysis of the Change in Microstructures of Nano Copper Powders During the Hydrogen Reduction using X-ray Diffraction Patterns and Transmission Electron Microscope, and the Mechanical Property of Compacted Powders. Journal of Korean Powder Metallurgy Institute, 2014, 21, 207-214.	0.2	0
748	Effect of Revolution on Inhomogeneous Deformation of IF Steel in High Pressure Torsion. Materials Sciences and Applications, 2016, 07, 673-679.	0.3	0
749	Analyses of Sever Plastic Deformation Behavior of Hot Isostatic Pressed Ni-base Superalloy during High Pressure Torsion Process. Transactions of Materials Processing, 2016, 25, 254-260.	0.1	0
750	Stretch-Flangeability of Harmonic Structure Material Manufactured by Powder Metallurgy Method. Journal of Korean Powder Metallurgy Institute, 2017, 24, 128-132.	0.2	0
751	Finite Element Analysis on the Effect of the Surface Roughness on the Tensile Properties of Pure Titanium. Transactions of Materials Processing, 2017, 26, 108-114.	0.1	0
752	Evaluation of the Reactivity of Bulk Nano Ni/Al Powder Manufactured by Shock Compaction Process. Transactions of Materials Processing, 2017, 26, 216-221.	0.1	0
753	Simulación del procesamiento de una aleación de Ti-6Al-7Nb por la técnica de presión en canal angular constante usando el método de elementos finitos. TecnologÃa En Marcha, 2017, 30, 25.	0.1	Ο